JOC The Journal of Organic Chemistry

pubs.acs.org/joc Article

Why [4 + 2 + 1] but Not [2 + 2 + 1]? Why Allenes? A Mechanistic Study of the Rhodium-Catalyzed [4 + 2 + 1] Cycloaddition of *In Situ* Generated Ene−Ene−Allenes and Carbon Monoxide

Yusheng Yang,[†] Zi-You Tian,[†] Chen-Long Li, and Zhi-Xiang Yu*

Cite This: *J. Org. Chem.* 2022, 87, 10576−10591 Read Online

ACCESS | Metrics & More | Article Recommendations | Supporting Information

ABSTRACT: Transition metal-catalyzed [4 + 2 + 1] cycloaddition of *in situ* generated ene/yne−ene−allenes (from ene/yne−ene propargyl esters) and carbon monoxide (CO) gives the [4 + 2 + 1] cycloadducts rather than [2 + 2 + 1] cycloadducts. Investigating the mechanism of this [4 + 2 + 1] reaction and understanding why the [2 + 2 + 1] reaction does not compete and the role of the allene moiety in the substrates are important. This is also helpful to guide the future design of new [4 + 2 + 1] cycloadditions. Reported here are the kinetic and computed studies of the [4 + 2 + 1] reactions of ene−ene propargyl esters and CO. A quantum chemical study (at the DLPNO-CCSD(T)//BMK level) revealed that the [4 + 2 + 1] reaction includes four key steps, which are 1,3-acyloxy migration (rate-determining step), oxidative cyclization, CO migratory insertion, and reductive elimination. The allene moiety in the substrates is critical for providing additional coordination to the rhodium center in the final step of the catalytic cycle, which in turn favors the reductive elimination transition state in the [4 + 2 + 1] rather than in the [2 + 2 + 1] pathway. The CO insertion step in the [4 + 2 + 1] reaction, which could occur through either the UP (favored here) or DOWN CO insertion pathway, has also been deeply scrutinized, and some guidance from this analysis has been provided to help the future design of new [4 + 2 + 1] reactions. Quantum chemical calculations have also been applied to explain why [4 + 2] and [4 + 1] cycloadditions do not happen and how trienes as side products for some substrates are generated.

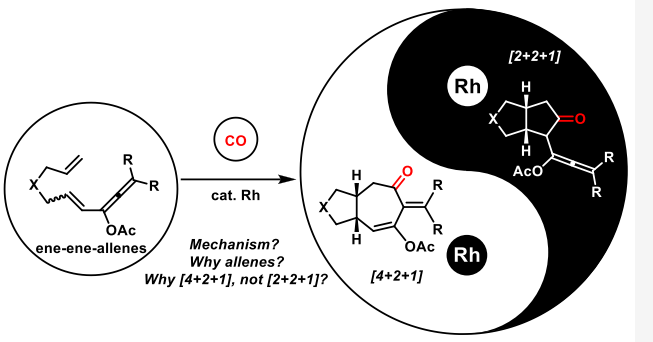

INTRODUCTION

Transition metal-catalyzed cycloadditions have evolved as powerful tools to access various ring skeletons that are widely found in natural products and pharmaceutical compounds.[1] Continuing efforts are required to develop more diverse cycloadditions to access cyclic molecules, which are not reachable, or need tedious transformations (for either substrate preparation or cycloadduct elaboration) if applying the reported known reactions. It is well known that seven-membered carbocyclic rings, which are widely found in natural products of biological activities, belong to the challenging medium-sized rings for synthesis,[2] and synthetic chemists still do not have many reactions and strategies at hand for choice when they are planning their syntheses of these target molecules and their analogs. For example, until now only a limited number of transition metal-catalyzed cycloaddition reactions can be used to synthesize seven-membered carbocycles directly.[1,3] Therefore, chemists have been endeavoring to discover and develop new transition metal-catalyzed cycloadditions for this purpose.

It is easily envisioned that a straightforward way to reach seven-membered carbocycles is to develop transition metal-catalyzed [4 + 2 + 1] cycloadditions of ene/yne/allene−dienes and carbon monoxide (CO), considering that the ene/yne/allene−diene substrates are easily synthesized, while carbon monoxide is cheap and abundant (Scheme 1a, yne/allene−dienes are not shown here).[4,5] However, these envisioned reactions are not guaranteed to give [4 + 2 + 1] products since either [4 + 2] or [2 + 2 + 1] products may be obtained from the proposed intermediates involved in the [4 + 2 + 1] reactions. The Wender group has investigated the reactions of ene/yne/allene−dienes and CO under rhodium catalysts, finding that these reactions mainly gave [2 + 2 + 1] cycloadducts, and only a minor [4 + 2 + 1] cycloadduct was obtained in one example (Scheme 1b).[4]

The abovementioned findings prompted us to hypothesize that, employing rhodium (or other transition metals) catalysts,

Received: February 22, 2022
Published: July 29, 2022

https://doi.org/10.1021/acs.joc.2c00406
J. Org. Chem. 2022, 87, 10576−10591

Scheme 1. (a) [4 + 2], [4 + 2 + 1], and [2 + 2 + 1] Cycloadditions and Two CO Insertion Pathways, (b) Wender's [2 + 2 + 1] Reactions of Ene/Yne/Allene−Dienes and Carbon Monoxide, Where [4 + 2 + 1] Was a Minor Product in One Example, and (c) Our Previously Reported [4 + 2 + 1] Cycloaddition

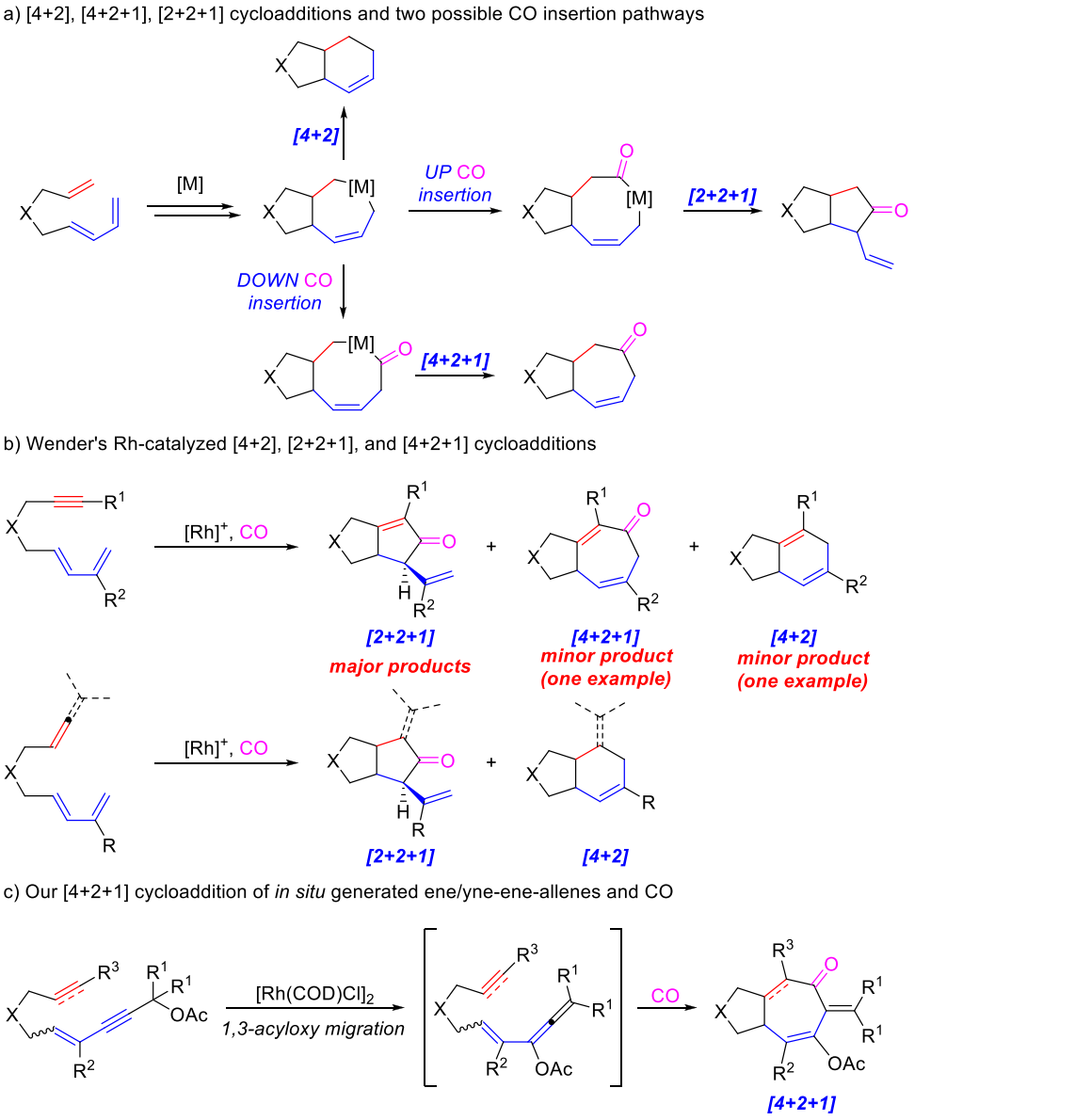

the reactions of ene/yne/allene−dienes and CO could intrinsically favor affording their corresponding [2 + 2 + 1] rather than [4 + 2 + 1] products. How can this "intrinsic" hurdle be overcome? In our opinion, there are possibly two strategies to realize the target [4 + 2 + 1] cycloadditions of ene/yne/allene−dienes and CO. The first strategy, the so-called catalyst searching strategy (**CSS**), is to find an appropriate catalyst (a combination of a transition metal (M) with/without a ligand (L)) to fulfill the goal; the second strategy, so-called here as a substrate-designing strategy (**SDS**) is to design some special but important substrates so that [4 + 2 + 1] cycloadditions, compared to their competing [2 + 2 + 1] cycloadditions, become preferred kinetically.

Adopting these two strategies to realize [4 + 2 + 1] cycloadditions requires not only experimental tests, but also a deep mechanistic understanding of successful [4 + 2 + 1] reactions reported. Fortunately, our group discovered a rhodium-catalyzed [4 + 2 + 1] cycloaddition of *in situ* generated ene/yne−ene−allenes from ene/yne−ene propargyl esters with CO, which can be regarded as a [4 + 2 + 1] cycloaddition using the **SDS** strategy (Schemes 1c and 2).[6] This new [4 + 2 + 1] reaction is efficient to get access to 5/7 fused rings, and several selected examples are given in Scheme 2a. Therefore, it is crucial to understand how this [4 + 2 + 1] cycloaddition takes place. It is also important to know the role of allenes in the *in situ* generated substrates in affecting the regiochemistry, considering that the ene/yne/allene−diene substrates, favoring [2 + 2 + 1] reactions (reported by Wender and co-workers), do not have this functional group in their diene moieties. The insights from the mechanistic studies will help the future development of new [4 + 2 + 1] cycloadditions via either the **CSS** or **SDS** strategy.

The proposed mechanisms of the [4 + 2 + 1] and other side reactions for ene/yne−ene−allenes and CO are shown in Scheme 3. In the [4 + 2 + 1] cycloaddition, the propargyl ester first undergoes Rh-catalyzed 1,3-acyloxy migration[7] to form

https://doi.org/10.1021/acs.joc.2c00406
J. Org. Chem. 2022, 87, 10576−10591

Scheme 2. (a) Selected Examples of [4 + 2 + 1] Cycloadditions and Side Products and (b) Model Reactions for Calculations

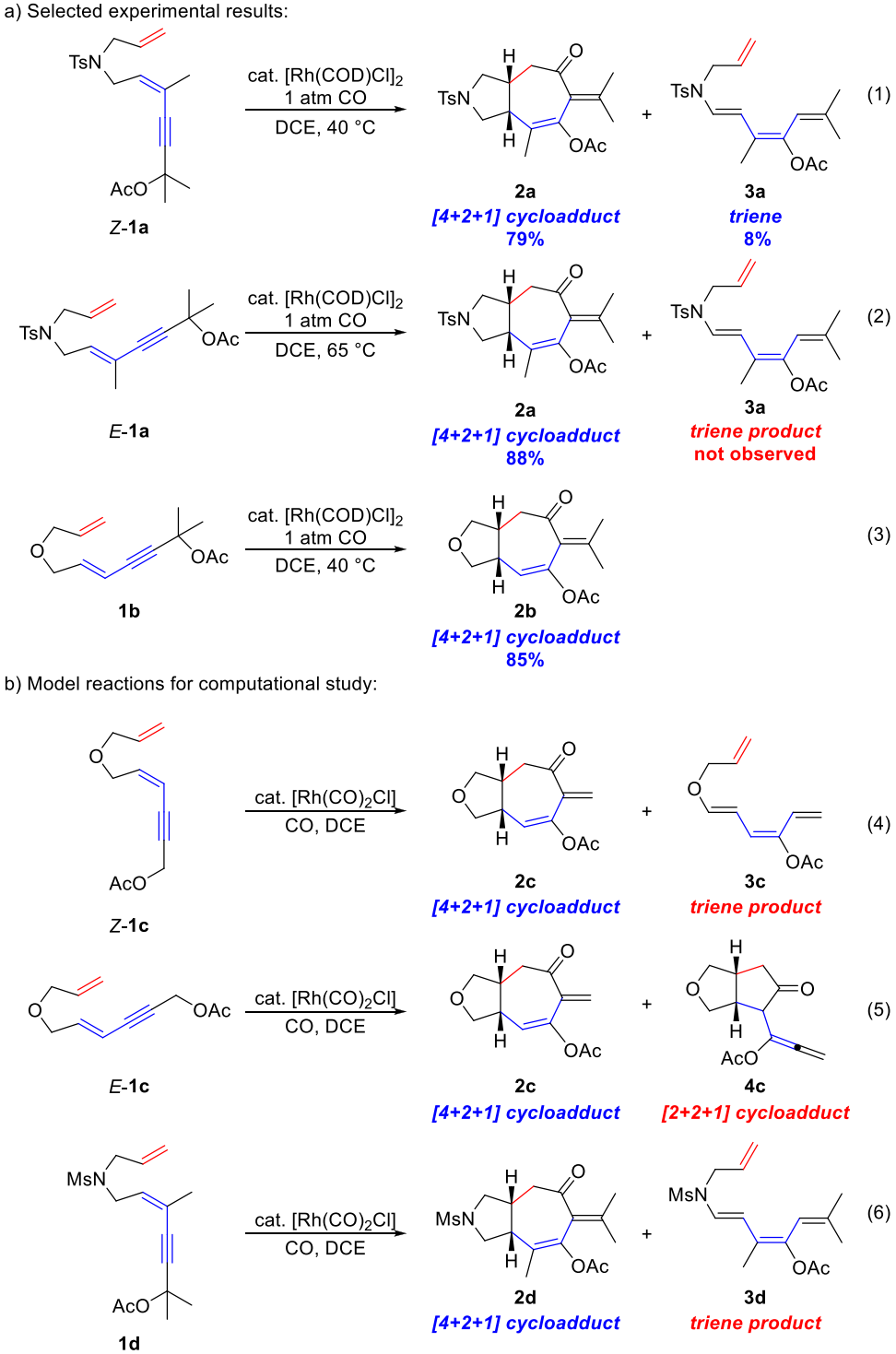

intermediate **I** with an allene moiety, which is followed by an intramolecular diene oxidative cyclization to generate a five-membered metallacycle, intermediate **II**. Then, the ene/yne component in the substrate inserts into the Rh−C bond in **II** to give intermediate **III**. In addition to this, intermediate **I** may undergo oxidative cycloaddition to form intermediate **III** in one step. Then, CO migratory insertion occurs to convert **III** into an eight-membered rhodacycle, intermediate **IV** or **IV′**, which subsequently undergoes reductive elimination to generate the desired [4 + 2 + 1] product. Several possible side reactions might compete from all possible intermediates in this [4 + 2 + 1] cycloaddition. For example, intermediate **II** may undergo a CO migratory insertion, followed by reductive elimination to give a [4 + 1] cycloaddition product.[8] Intermediate **III** may directly undergo a reductive elimination to produce a [4 + 2] cycloaddition product.[9,10] In addition, we experimentally discovered that a side reaction occurred, generating trienes when *Z*-ene−ene propargyl esters were used (see more information below, together with the correction of the stereochemistry of the side product in the

https://doi.org/10.1021/acs.joc.2c00406
J. Org. Chem. 2022, 87, 10576−10591

Scheme 3. Proposed Mechanisms of [4 + 2 + 1] Cycloaddition and Possible Side Reactions

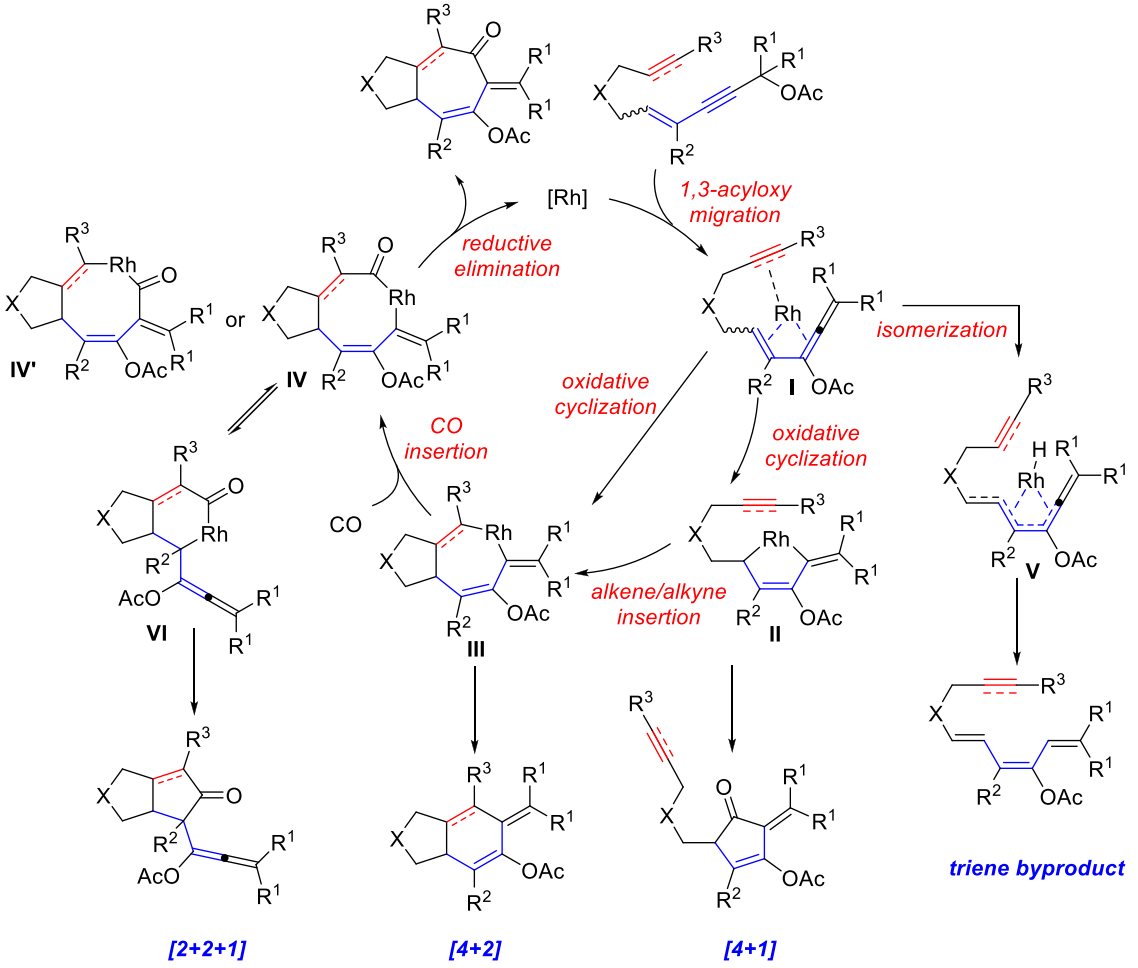

Revision of the Geometry of the Triene Side Products section). We previously postulated that the formation of trienes involves C−H activation and reductive elimination from the allene intermediate **I**. This needs to be supported or disputed by further mechanistic study. In addition, intermediate **IV** may be transformed into intermediate **VI**, which could then undergo a different reductive elimination (compared to that in the [4 + 2 + 1] cycle) to form a Pauson−Khand [2 + 2 + 1] product.[4] Experimentally, [2 + 2 + 1] products were not observed, but some triene byproducts and trace amounts of [4 + 2] cycloadducts were found. We point out that another pathway[6a] starting from ene−ene oxidative cyclization, which is followed by several other steps to the final [4 + 2 + 1] product, had also been studied computationally, revealing that this pathway was disfavored compared to that discussed in the main text, and therefore this is discussed only in the Supporting Information.

In what follows, we report our experimental and computational study of the reaction mechanisms and understanding of regiochemistry, the role of allenes in the [4 + 2 + 1] reaction, together with some suggestions for the future design of new [4 + 2 + 1] reactions.

COMPUTATIONAL DETAILS

DFT calculations were performed using Gaussian 09 E.01.[11] DLPNO-CCSD(T)[12] single-point energy calculations were performed using ORCA 4.2.1.[13] Pruned integration grids with 99 radial shells and 590 angular points per shell were used in DFT calculations (int=ultrafine). Geometry optimization of all of the minima and transition states was carried out with the BMK functional[14] at 298 K in the gas phase, and the def2-SVP[15] basis set was used for all atoms. The BMK functional performed well in our previous benchmark study of the $[Rh(CO)_2Cl]_2$-catalyzed [5 + 2 + 1] cycloaddition of ene−VCPs and CO and was chosen in the present study as well.[16] Vibrational frequencies were computed at the same level to check whether each optimized structure was an energy minimum or a transition state. Zero-point vibrational energies were obtained through frequency calculations. Solvent effects were considered based on gas-phase-optimized structures using the same basis set and functional. Solvation energies in 1,2-dichloroethane were evaluated by a self-consistent reaction field employing an SMD model.[17] Based on the optimized structures, single-point energy refinements were performed at the DLPNO-CCSD(T)/def2-TZVPP[15] level (def2-TZVPP/C auxiliary basis set) with TightSCF and TightPNO keywords. In this paper, all discussed energies are Gibbs free energies in the solution phase (ΔG_{sol}, at 298 K) unless otherwise specified. We have searched for all possible conformers for all intermediates and transition states, and the discussed ones in this paper are the most stable. The standard state for CO is 5.5 mM[18] and the other species have standard states of 1.0 M.[19] All 3D structures were prepared using CYLview20.[20]

https://doi.org/10.1021/acs.joc.2c00406
J. Org. Chem. 2022, 87, 10576−10591

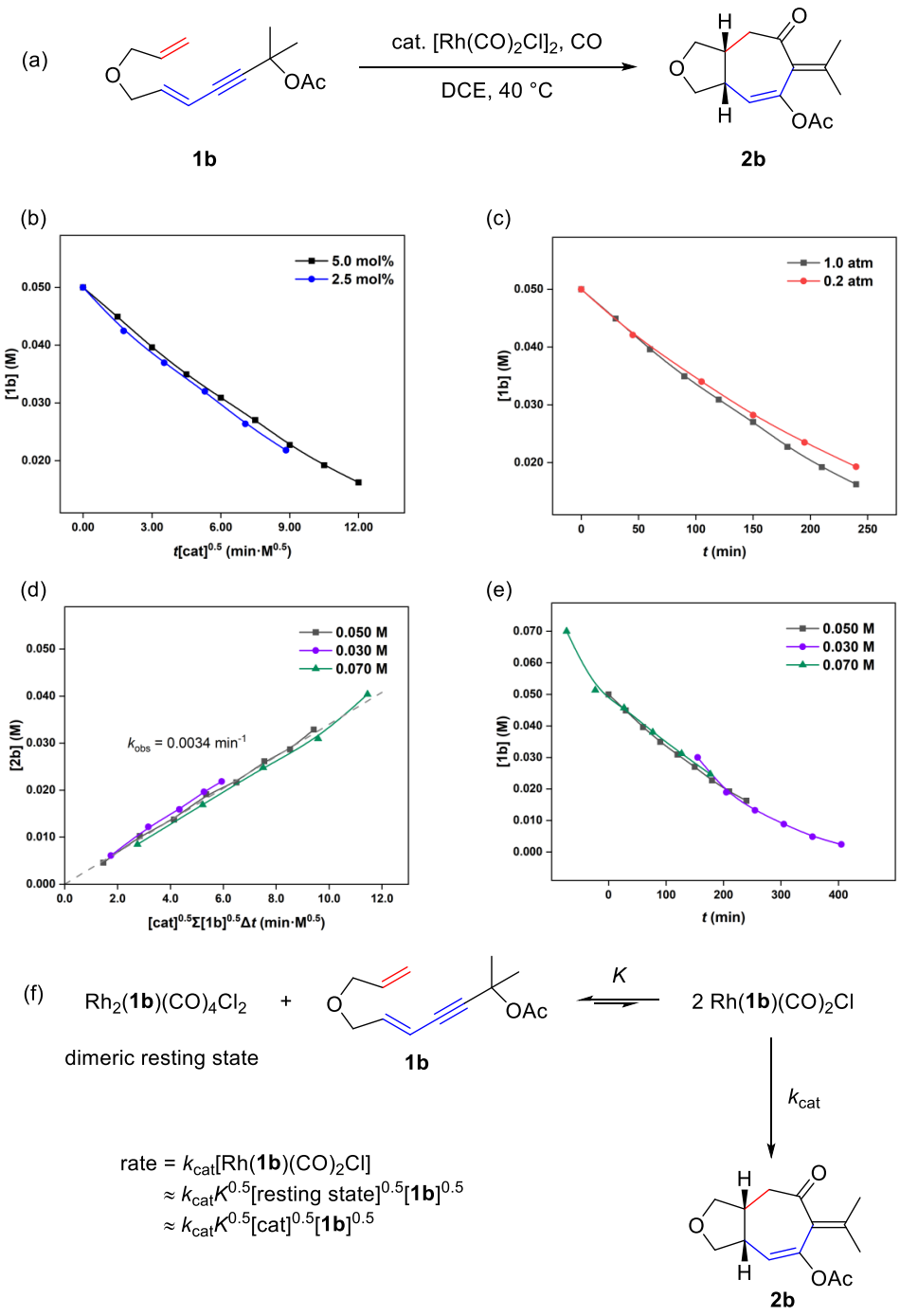

Figure 1. Visual kinetic analysis on (a) the cycloaddition of substrate **1b** and CO. Reaction conditions: (b) **1b** (0.050 M), $[Rh(CO)_2Cl]_2$ (5.0; 2.5 mol %), CO (1.0 atm), DCE, 40 °C. (c) **1b** (0.050 M), $[Rh(CO)_2Cl]_2$ (5.0 mol %), CO (0.2 atm; 1.0 atm), DCE, 40 °C. (d) **1b** (0.030; 0.050; 0.070 M), $[Rh(CO)_2Cl]_2$ (5.0 mol %), CO (1.0 atm), DCE, 40 °C. (e) **1b** (0.030; 0.050; 0.070 M), $[Rh(CO)_2Cl]_2$ (5.0 mol %), CO (1.0 atm), DCE, 40 °C. (f) Proposed rate law and dimeric resting state based on experimental kinetic data and calculations.

RESULTS AND DISCUSSION

Kinetic Study of the [4 + 2 + 1] Reaction. Experimentally, our [4 + 2 + 1] cycloaddition had a broad scope and the tethers of the substrates can be $C(CO_2Me)$, O, and TsN. The catalyst for this reaction can be either $[Rh(COD)Cl]_2$, $[Rh(COE)_2Cl]_2$, or $[Rh(CO)_2Cl]_2$ because all of them gave almost similar [4 + 2 + 1] cycloaddition results[6a] (83, 82, and 81% reaction yields, respectively, for one substrate with the TsN-tether). Therefore, we proposed that under a 1 atm CO atmosphere, all of these precatalysts may undergo ligand exchange with CO to form $[Rh(CO)_2Cl]$, which could enter the catalytic cycle as a monomer (there are also possibilities of the initiation of the catalytic cycle. However, these details are not critical for understanding the key [4 + 2 + 1] cycloaddition). Here, we report our measured kinetic data for this reaction using the catalyst of $[Rh(CO)_2Cl]_2$ to get more mechanistic information about the reaction.

Employing an O-tether substrate **1b**, visual kinetic analysis was performed to investigate reaction orders in the catalyst,

https://doi.org/10.1021/acs.joc.2c00406
J. Org. Chem. 2022, 87, 10576−10591

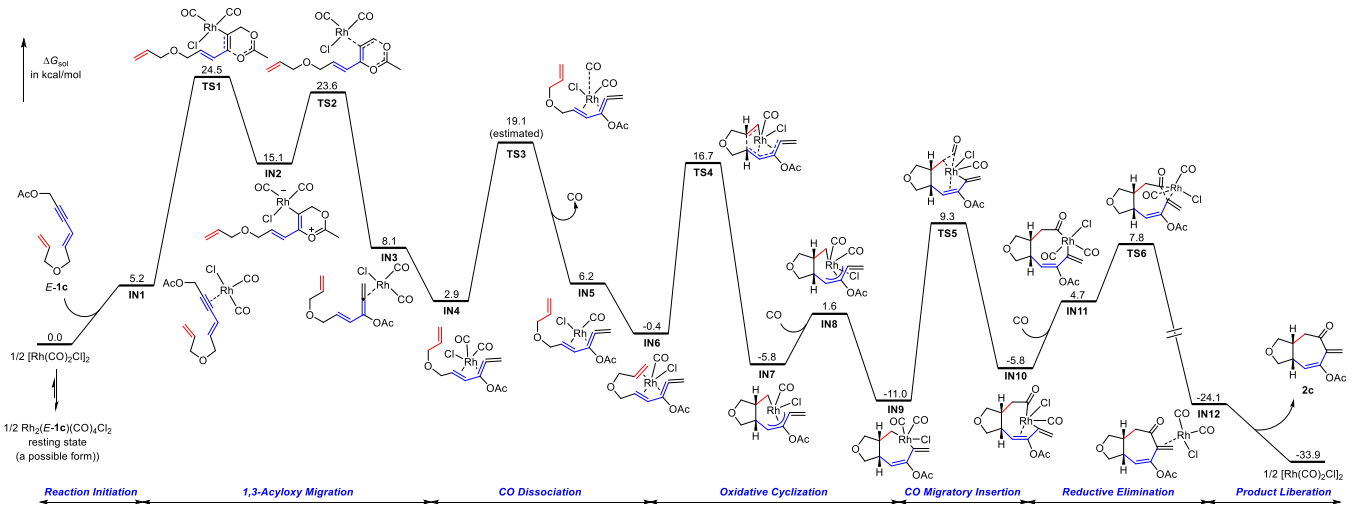

Figure 2. Gibbs free energy profile of the [4 + 2 + 1] cycloaddition of *E*-**1c** and CO (the generation of **IN1** from the resting state is just schematically presented for understanding).

substrate, and CO by monitoring ^{1}H NMR spectroscopy in the [4 + 2 + 1] reaction, which was then analyzed by a normalized time scale method and variable time normalization analysis (Figure 1).[21] We found that the [4 + 2 + 1] cycloaddition is the 0.5th order in $[Rh(CO)_2Cl]_2$, 0th order in CO, and 0.5th order in the substrate (Figure 1b–d). The 0.5th order in the catalyst suggests that there exists an equilibrium between a dimeric off-cycle resting state and a monomeric catalytic species. The 0.5th order in substrate **1b** suggests that the resting state contains two rhodium centers and one molecule of the substrate, whereas the catalytic species includes one rhodium center and one substrate. The 0th order in CO indicates that the number of CO ligands in the resting state is twice as many as that in the turnover-limiting transition state. We also found that the catalyst was not deactivated during the reaction (Figure 1e). Based on the kinetic data and calculations shown below, we proposed the possible dimeric resting-state Rh_2(**1b**)$(CO)_4Cl_2$ (solvent or other species could also be involved and the exact form of this is unknown) and another substrate to give substrate-$Rh(CO)_2Cl$ species, which then directly undergo 1,3-acyloxy migration as the rate-determining step of the catalytic cycle. Therefore, we proposed the rate law of this [4 + 2 + 1] reaction for **1b** and CO, shown in Figure 1f (the [cat] is the concentration of $[Rh(CO)_2Cl]_2$). The plot of different concentrations of **1b** shows overlaid straight curves with a slope of 0.0034 min^{-1}, which corresponds to k_{obs} for this reaction (Figure 1d). This means that the present [4 + 2 + 1] reaction behaves like a reaction with a Gibbs free energy of activation of ca. 23.5 kcal/mol, estimated using the Eyring equation. We cannot get the equilibrium constant K in Figure 1f, so we cannot compare this measured value with the computed one, considering that $k_{obs} = k_{cat}K^{0.5}$. The kinetic process of the present [4 + 2 + 1] reaction is similar to the [5 + 2 + 1] reaction reported by our group.[16]

Gibbs Free Energy Profile of the [4 + 2 + 1] Reaction from *Ab Initio* Calculations. Simplified model reactions of 4 and 5 (Scheme 2b) were employed to answer the above-mentioned mechanistic questions aided by quantum chemical calculations. The difference between *Z*-**1c** and *E*-**1c** in these model reactions is the configuration of the internal double bond. Therefore, we can study the reactions of these two substrates to understand how the geometry of the alkene in ene–allene moieties affects the reaction. To better understand the regiochemistry, reaction 6 with **1d** as the substrate (shown in Scheme 2) has also been investigated, where only the key steps involving the regiochemistry issue had been computed and discussed (see the Supporting Information).

Figure 2 describes the Gibbs free energy profile of the [4 + 2 + 1] cycloaddition starting from the substrate-$Rh(CO)_2Cl$ complex, **IN1**, which is proposed to be generated by the process shown in Figure 1f. The catalytic cycle of the [4 + 2 + 1] reaction constitutes four steps: 1,3-acyloxy migration of an ester group, oxidative cyclization, CO migratory insertion, and reductive elimination. We describe all steps in detail.

Ligand Exchange and 1,3-Acyloxy Migration. The 1,3-acyloxy migration reaction transforms the studied substrate complex **IN1** into its corresponding allene intermediate **IN3**. The carbonyl oxygen atom in complex **IN1**, acting as a nucleophile, attacks the activated alkyne via **TS1** to form intermediate **IN2**. This step requires a Gibbs free energy of activation of 19.3 kcal/mol. The second step in the 1,3-acyloxy migration process is to break the C–O bond to give the rhodium–allene complex **IN3**, requiring a Gibbs free energy of activation of 8.5 kcal/mol via **TS2**. The whole process of 1,3-acyloxy migration from intermediate **IN1** to intermediate **IN3** is endergonic by 2.9 kcal/mol in terms of Gibbs free energy. **TS1** is the rate-determining transition state in this migration step. Similar DFT studies of 1,3-acyloxy migration have been investigated.[7] We point out here that the direct 1,3-acyloxy migration without a catalyst is difficult, requiring 42.5 kcal/mol of activation free energy (see the Supporting Information).

CO Dissociation. Intermediate **IN3** is a 16-electron complex, which can be converted into a more stable 18-electron complex **IN4** through coordination of Rh by the diene moiety. Intermediate **IN4** can dissociate a CO molecule to form intermediate **IN5**, which subsequently can be coordinated by a double bond in this intermediate, forming an 18-electron complex **IN6**. We could not locate a transition state for CO dissociation (**TS3**) because this is an uphill process electronically. Therefore, we estimate this process through the single-point energy calculation by scanning the Rh–CO bond length, finding that the electronic energy for CO dissociation is 16.2 kcal/mol. Therefore, the upper value of **TS3** is ca. 16.2 kcal/mol (the actual activation free energy should be lower

https://doi.org/10.1021/acs.joc.2c00406
J. Org. Chem. 2022, 87, 10576–10591

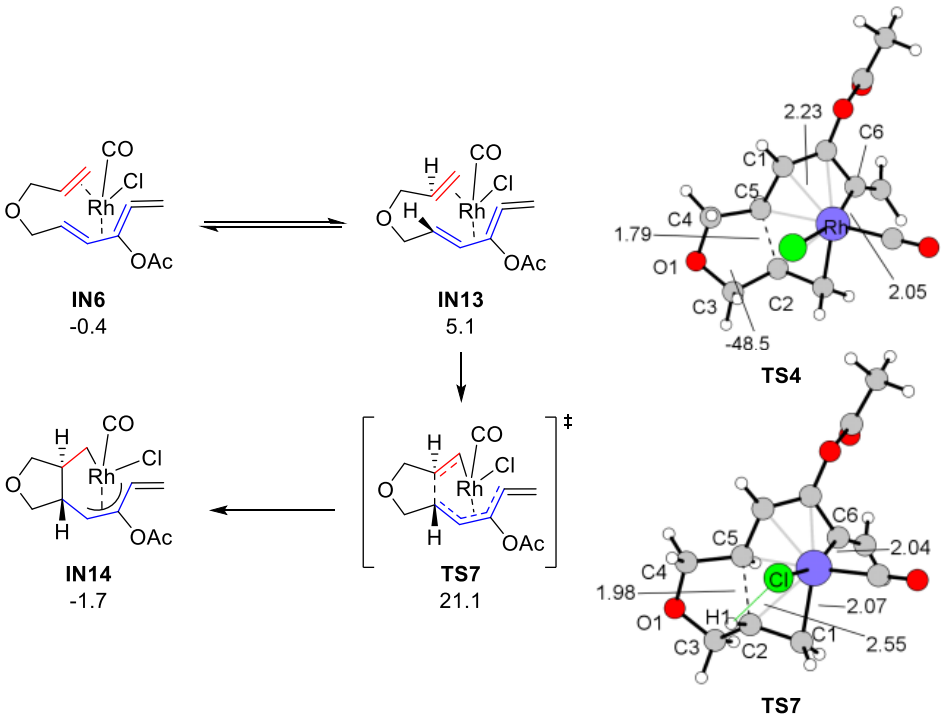

Figure 3. Oxidative cyclization and the corresponding *cis*- and *trans*-oxidative cyclization transition states.

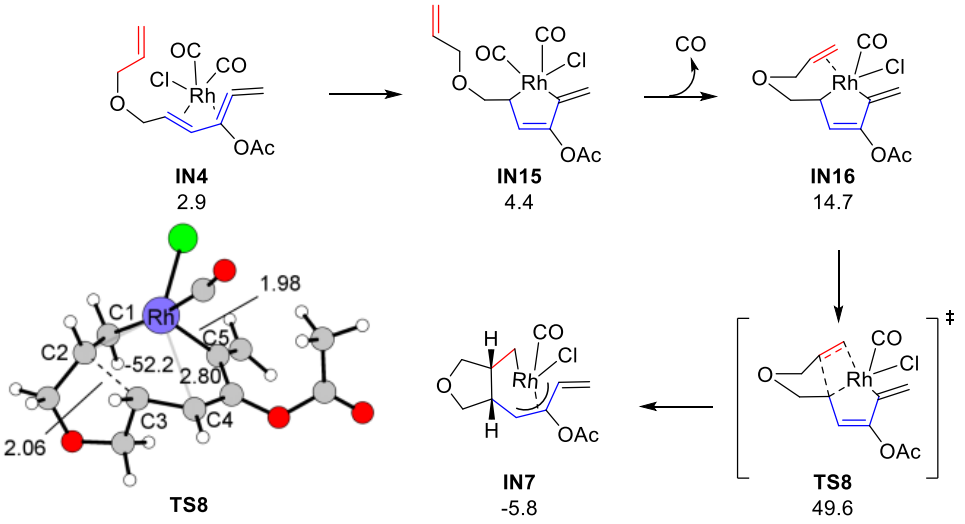

Figure 4. Disfavored alkene insertion pathway and the corresponding transition state.

than this value if entropy contribution is considered). Therefore, CO dissociation is an easy process in the present reaction.

Oxidative Cyclization. The oxidative cyclization, which is undertaken by intermediate **IN6**, then constructs the seven-membered rhodacycle of intermediate **IN7** via **TS4**, simultaneously setting two stereocenters at the bridgehead positions (Figure 3). In **TS4**, the forming C2−C5 bond length is 1.79 Å, while the lengths of the forming C6−Rh and C1−Rh bonds are 2.05 and 2.23 Å, respectively. From intermediate **IN6** to intermediate **IN7**, the *cis*-oxidative cyclization reaction requires 17.1 kcal/mol of Gibbs free energy.

The *trans*-oxidative cyclization via the transition state **TS7** requires 21.5 kcal/mol of Gibbs free energy (from **IN6**) to generate intermediate **IN14** (Figure 3). Two factors are responsible for the higher Gibbs free energy of **TS7** compared with **TS4**. First, **TS7** adopts a half-chair five-membered ring conformation and experiences more distortion than the corresponding five-membered ring with an envelope conformation in **TS4**. The dihedral angle of C2−C3−O1−C4 in **TS7** is 24.3°, whereas this is 48.5° in **TS4**. The second factor is the steric repulsion between the inner hydrogen atom in the alkene and the chlorine ligand in **TS7**. This distance between them is 2.55 Å, much less than the sum of the van der Waals radius of hydrogen and chlorine atoms, 2.95 Å.

After the formation of intermediate **IN7**, a CO molecule coordinates with the rhodium atom in intermediate **IN7**, forming an 18-electron intermediate **IN8**. Intermediate **IN8** is less stable than intermediate **IN7** by 7.4 kcal/mol in terms of Gibbs free energy. However, it can then undergo a geometric change by removing the coordination from a double bond, giving a more stable 16-electron intermediate **IN9**.

https://doi.org/10.1021/acs.joc.2c00406
J. Org. Chem. 2022, 87, 10576−10591

Scheme 4. Mechanistic Rationale to Understand CO Coordination and Regiochemistry of [4 + 2], [4 + 2 + 1], and [2 + 2 + 1] Cycloadditions

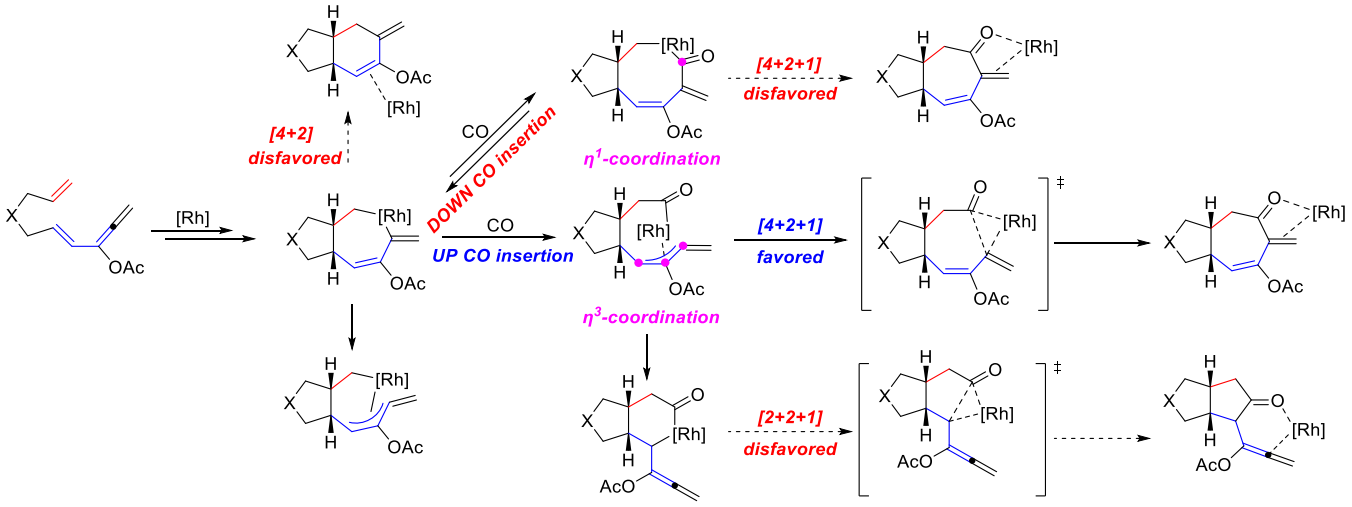

We have also considered another possible pathway to form intermediate **IN7** via oxidative cyclization and alkene insertion (Figure 4). This alkene insertion pathway is kinetically disfavored. Oxidative cyclization of vinyl allene forms the five-membered rhodacycle intermediate **IN15**, which has a planar structure with two CO molecules coordinated. Then, CO dissociation and coordination by the terminal alkene of the substrate generate the 16-electron complex **IN16**. The alkene insertion step via **TS8** requires 34.9 kcal/mol in terms of Gibbs free energy, higher than **TS4** by 32.9 kcal/mol. As a result, this pathway can be excluded from further consideration.

TS8 is disfavored for two reasons. The first reason is that there are ring distortions in **TS8**. The four-membered rhodacycle in **TS8** is seriously distorted with a 52.2° dihedral angle of Rh−C1−C2−C3. Usually, alkene insertion into the C−M bond prefers to have a planar four-membered ring transition state, as indicated by Morokuma.[22] The second reason is attributed to the coordination effect. Due to the five-membered ring's restriction, the bond length of Rh−C5 is 1.98 Å, whereas the Rh−C4 bond is 2.80 Å. The 0.82 Å difference between these two bond lengths suggests that the alkene group does not coordinate with rhodium tightly.

CO Insertion (UP CO Insertion vs DOWN CO Insertion) and Reductive Elimination. In connection with intermediates **IN9**, two CO migrative insertion transition states, **TS5** and **TS9** can be located, which belong to two pathways, named UP and DOWN CO insertion pathways for easier description (see these in Scheme 4). Intermediate **IN8** with an η^3-coordination can isomerize into a more stable complex **IN9** with an η^1-coordination by removing the coordination of a double bond (this step is exergonic by 12.6 kcal/mol due to a release of the ring strain). In **TS5**, the carbonyl group is inserted into the Csp^3−Rh bond (UP CO insertion). The CO migratory insertion via **TS5** requires a Gibbs free energy of activation of 20.3 kcal/mol from intermediate **IN9**.

To realize the DOWN CO insertion via **TS9**, the carbonyl group in **IN9** is inserted into the Csp^2−Rh bond, converting intermediate **IN9** into intermediate **IN17** with a Gibbs free energy of activation of 21.1 kcal/mol. **TS5** is lower than **TS9** by 0.8 kcal/mol in terms of Gibbs free energy. It is important to point out that the CO insertion reactions are irreversible in the UP CO insertion pathway and reversible in the DOWN CO insertion pathway. In the UP CO insertion pathway, the followed step via **TS6**, corresponding to the reductive elimination transition state to generate the [4 + 2 + 1] product, is lower in energy than **TS5**, indicating that this CO insertion step is irreversible and **TS4** is responsible for determining whether CO insertion chooses the UP or DOWN pathway. In the DOWN CO insertion pathway via **TS10**, the reductive elimination transition state for the formation of the [4 + 2 + 1] product (Figure 5) is higher in Gibbs free energy than **TS9** by 4.1 kcal/mol, suggesting that this CO insertion step is reversible and the reductive elimination transition state **TS10** is responsible for the regiochemistry of CO insertion. Therefore, we have to compare the relative energies of **TS5** (UP CO insertion pathway) and **TS10** (in the DOWN CO insertion pathway) to judge the regiochemistry. **TS5** is lower than **TS10** in terms of free energy by 4.9 kcal/mol, suggesting that UP CO insertion is exclusively favored based on the Curtin−Hammett principle. The UP CO insertion pathway can give either [4 + 2 + 1] products or [2 + 2 + 1] products, which will be analyzed in the subsequent session.

The major reason for the preference of the UP CO insertion transition state **TS5** is that **TS9** does not possess an η^3-coordination by the allylic ligand and behaves as a 14-electron complex, whereas **TS5** is a 16-electron complex due to the existence of an allylic η^3-coordination. This selectivity can be reflected by the thermodynamics of CO insertions. Intermediate **IN10** is thermodynamically more stable than intermediate **IN17** by 10.5 kcal/mol. In the intermediate **IN10**, the rhodium atom has an η^3-coordination of the allylic ligand, whereas intermediate **IN17** does not have this type of coordination.

The final step of the [4 + 2 + 1] cycloaddition in the major UP CO insertion pathway is the reductive elimination. First, CO coordinates with the 16-electron intermediate **IN10** to give again a 16-electron intermediate **IN11**, in which the coordination mode of the allyl ligand changes from η^3 to η^1. Then, intermediate **IN11** undergoes reductive elimination, requiring a Gibbs free energy of activation of 3.1 kcal/mol via **TS6**. In **TS6**, the forming C1−C2 bond length is 1.98 Å (Figure 5). We also considered other modes of this reductive elimination, which are all disfavored (see Figure S8).

https://doi.org/10.1021/acs.joc.2c00406
J. Org. Chem. 2022, 87, 10576−10591

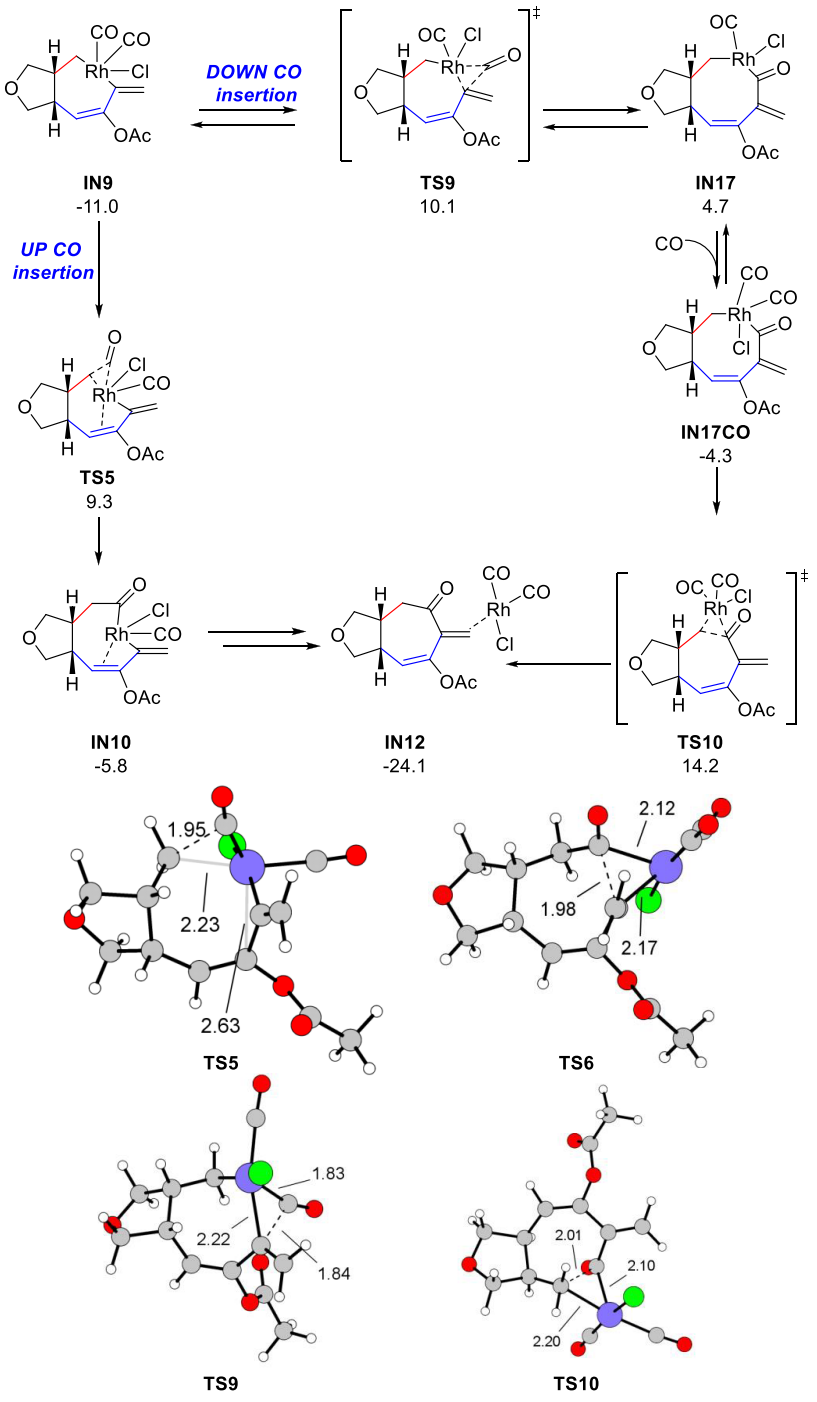

Figure 5. CO migratory insertion steps and the corresponding reductive elimination transition states.

Liberation of the [4 + 2 + 1] Product and Initiating the Next Catalytic Cycle. Intermediate **IN12**, which is a complex between the [4 + 2 + 1] cycloadduct and catalytic species of $Rh(CO)_2Cl$, could then undergo ligand exchange to liberate the cycloadduct, together with $Rh(CO)_2Cl$, which then forms the resting state with another $Rh(CO)_2Cl$ and substrate. With another incoming substrate, the [4 + 2 + 1] reaction can then continue a new catalytic cycle as shown in Figure 2.

Summary of the Mechanism of the [4 + 2 + 1] Cycloaddition. To sum up, the catalytic cycle of the [4 + 2 + 1] cycloaddition constitutes several elementary steps. It starts from the ligand exchange, followed by 1,3-acyloxy migration of an ester group to generate an ene−ene−allene intermediate. Then, CO dissociation takes place, followed by oxidative cyclization to generate a 5/7 rhodacyclic ring intermediate. After that, CO migratory insertion into the Csp^3−Rh bond (UP CO insertions) and reductive elimination from intermediate **IN11** give the [4 + 2 + 1] cycloadduct. The alkene insertion step determines the fused ring's stereochemistry. Two steps in the catalytic cycle are the most difficult, one is 1,3-acyloxy migration via **TS1** (19.3 kcal/mol) and the other is CO insertion via **TS5** (20.3 kcal/mol). The exact form of the resting state of this reaction is not known, but certain energy is required from the resting state to **IN1**. In this case, the rate-determining step in the [4 + 2 + 1] reaction is

https://doi.org/10.1021/acs.joc.2c00406
J. Org. Chem. 2022, 87, 10576−10591

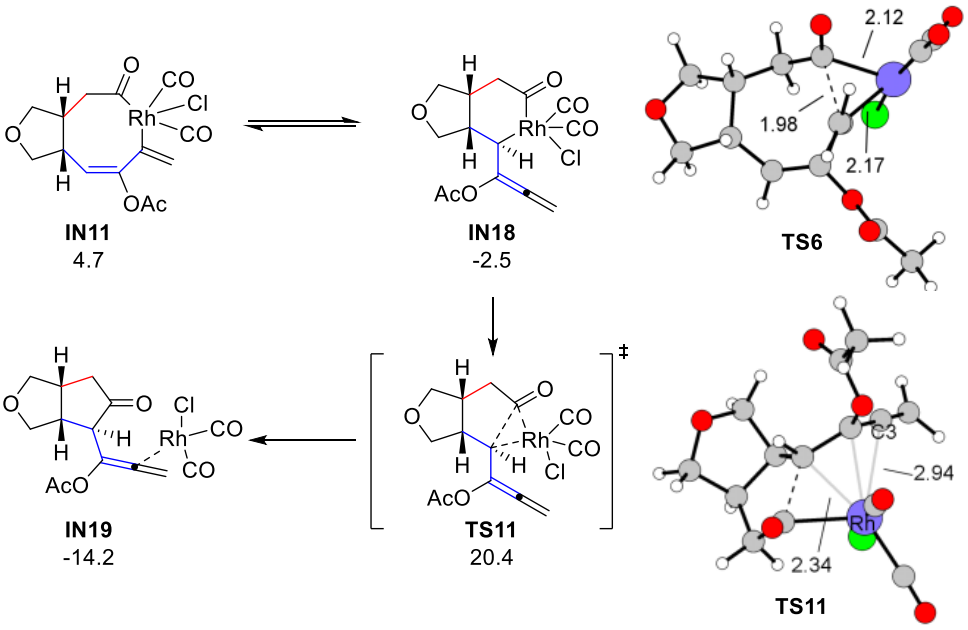

Figure 6. Reductive elimination transition states of [4 + 2 + 1] and [2 + 2 + 1] cycloadditions.

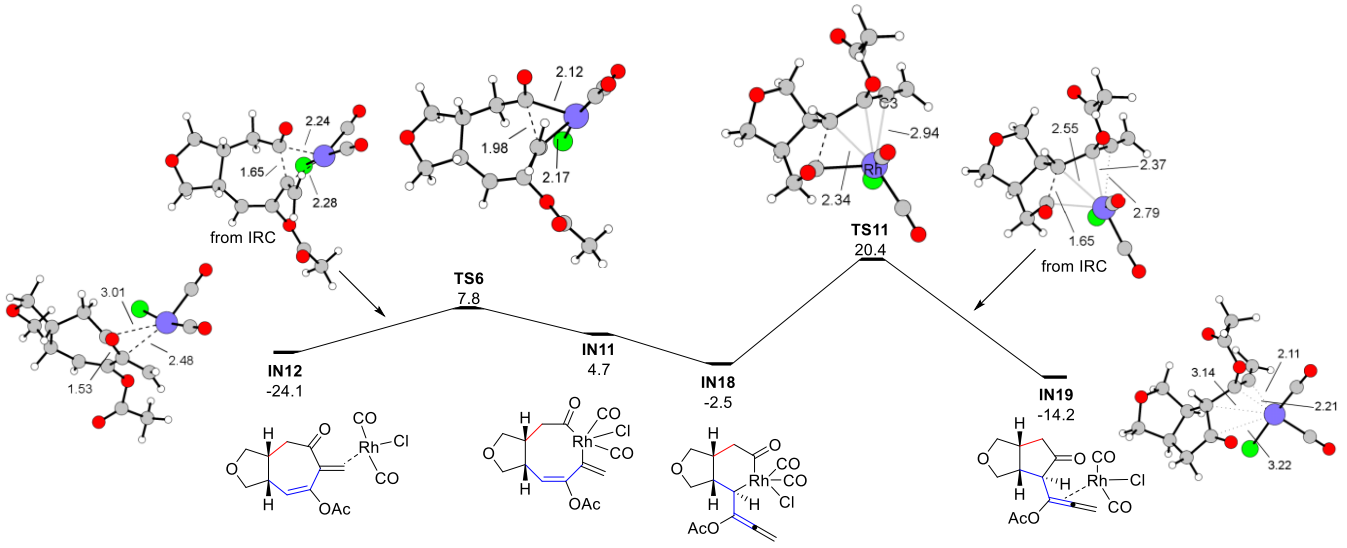

Figure 7. Intrinsic Reaction Coordinate (IRC) pictures of **TS6** and **TS11** to understand the coordination mode of rhodium atoms.

the 1,3-acyloxy migration. This is also suggested by the kinetic study mentioned above.

The computed overall activation free energy of the present [4 + 2 + 1] reaction is more than 24.5 kcal/mol (because we do not know how much free energy is needed from the resting state to $1/2[Rh(CO)_2Cl]_2$, which goes to **TS1** with the substrate requiring 24.5 kcal/mol). The calculation result can reflect the experimental observation that the reaction of **1b** (the real reaction) took place at 40 °C (Scheme 2).

Why Is the [2 + 2 + 1] Cycloaddition Disfavored? We also computed the potential energy surface of the [2 + 2 + 1] cycloaddition (Figure 6) to understand why this pathway is not favored. Intermediate **IN11** can isomerize without a barrier to intermediate **IN18**, indicated by quantum chemical calculations (see details in the Supporting Information). Intermediate **IN18** is a 16-electron complex, yet it is more stable than intermediate **IN11** by 7.2 kcal/mol in terms of Gibbs free energy.

Intermediate **IN18** can undergo a reductive elimination reaction via **TS11** to give the [2 + 2 + 1] product with an activation free energy of 26.2 kcal/mol (from intermediate **IN10**). **TS11** is higher than **TS6** in the [4 + 2 + 1] pathway, suggesting that [2 + 2 + 1] cycloaddition is disfavored according to the Curtin−Hammett principle. We also considered other modes of this reductive elimination (see Figure S10). This computational prediction is consistent with our experimental observations. The major reason for this regioselectivity is that the allene moiety in **TS11** does not coordinate with the rhodium atom, as indicated by the long distance between Rh and C3 atoms (2.93 Å). Therefore, in this transition state, the rhodium atom does not experience an η^3-coordination (leading to a 14-electron complex), making this process difficult. In contrast, the reductive elimination

https://doi.org/10.1021/acs.joc.2c00406
J. Org. Chem. 2022, 87, 10576−10591

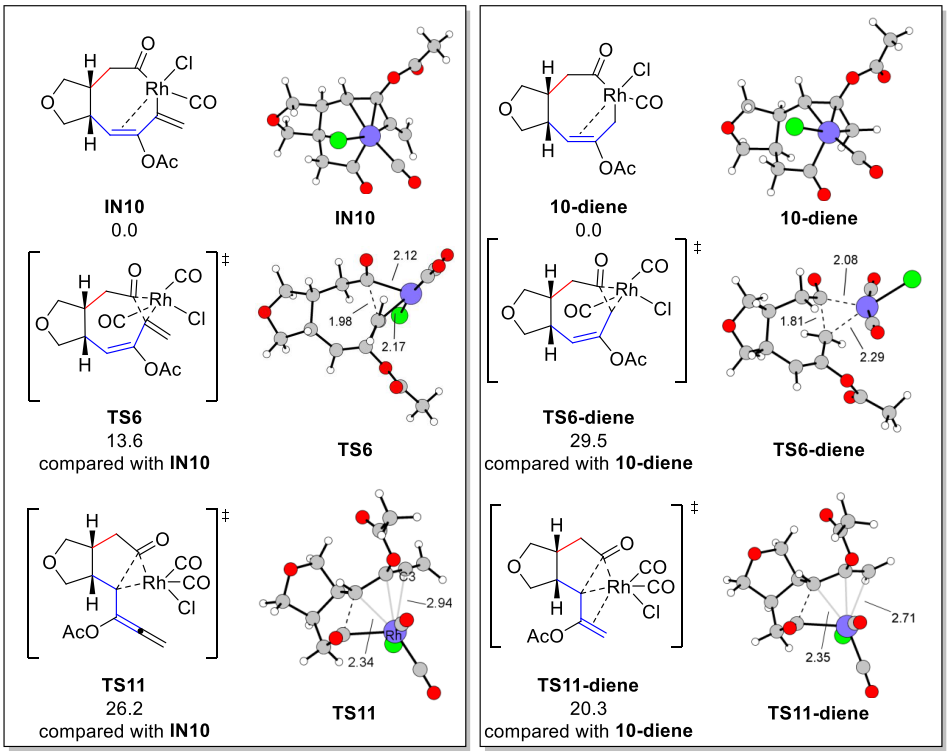

Figure 8. Understanding the role of an allene in affecting the regiochemistry of ([4 + 2 + 1] vs [2 + 2 + 1]) by comparing the reactions of *E*-**1c** and a hypothetic substrate of ene−diene (see the text).

Scheme 5. Reductive Elimination in the [4 + 2] Pathway Compared to the CO Insertion Step in the [4 + 2 + 1] Pathway

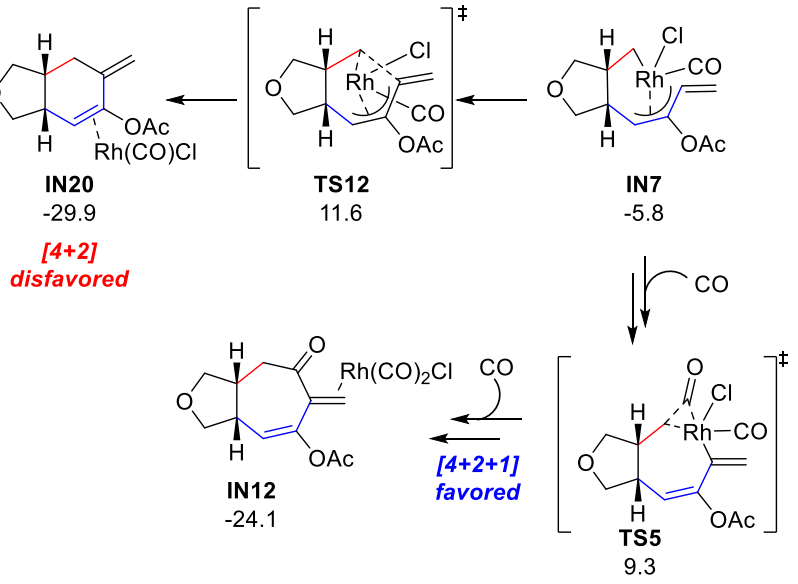

transition state **TS6** is a 16-electron complex, in which both carbon atoms of the forming C−C bond are of sp^2-hybridization, which can promote reductive eliminations. The intrinsic reaction coordinate (IRC) path results give support to this interpretation (Figure 7).

The cycloadditions of ene−dienes with CO prefer to give [2 + 2 + 1] products instead of [4 + 2 + 1] products, as indicated by Wender's report (Scheme 1b). Calculations were carried out to understand why the ene−allene moiety in our case is different from the diene moiety in Wender's substrate. These two situations were compared through hypothetic models (Figure 8). In our *in situ* generated yne/ene−allene [4 + 2 + 1] cycloadditions, **TS11** is higher than **TS6** by 12.6 kcal/mol in terms of free energy of activation, indicating that the [4 + 2 + 1] pathway is favored. In the ene−diene substrates, however, **TS11-diene** is lower than **TS6-diene** by 9.2 kcal/mol in terms of the activation of Gibbs free energy, indicating that the [2 + 2 + 1] cycloaddition pathway is favored for the mode system of ene−diene. The bond lengths of Rh−C3 are 2.94 Å in **TS11** and 2.71 Å in **TS11-diene**, indicating that an η^3-coordination exists in **TS11-diene** and only an η^1-coordination exists in **TS11**. This suggests that the allene in our case is very critical

https://doi.org/10.1021/acs.joc.2c00406
J. Org. Chem. 2022, 87, 10576−10591

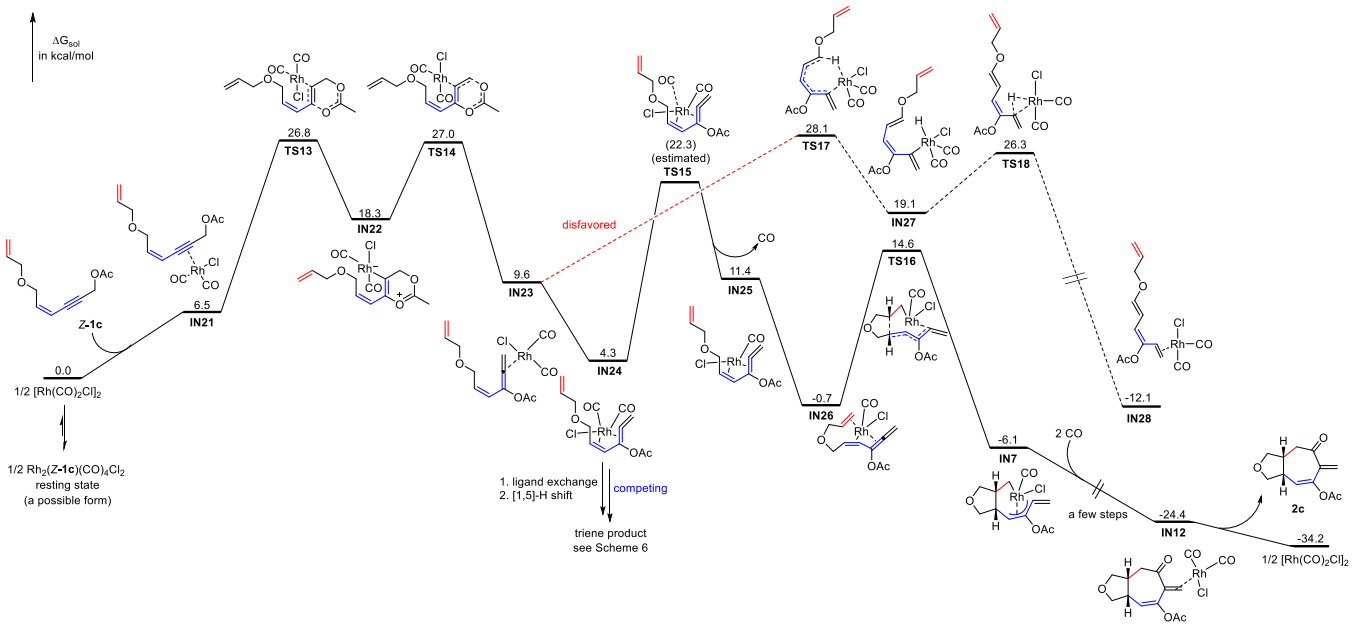

Figure 9. Gibbs free energy profiles of triene's generation and the [4 + 2 + 1] cycloaddition of *Z*-**1c** and CO (the generation of **IN21** from the resting state is just schematically presented for understanding).

for adding extra coordination, which consequently helps the [4 + 2 + 1] cycloaddition.

Here, we make two further comments. One is reductive elimination in the [4 + 2 + 1] pathway for the ene−diene system is more difficult than its counterpart in the ene−ene−allene system, as shown in Figure 8. This is because the reductive elimination transition state **TS6-diene** in the former forms a $C(sp^2)-C(sp^3)$ bond and its rhodium is of a 14-electron complex, while the reductive elimination transition state **TS6** in the latter forms a $C(sp^2)-C(sp^2)$ bond and its rhodium is of a 16-electron complex (one of the sp^2 carbon can coordinate with rhodium).[23] In contrast, the reductive elimination in the [2 + 2 + 1] pathway for the ene−diene system is easier than its counterpart in the ene−ene−allene system, as shown in Figure 8. This is because the reductive elimination transition state **TS11-diene** in the former benefits coordination from the forming external alkene, but **TS11** does not have this coordination from the forming external allene.

Some Insights for Guiding the Design of [4 + 2 + 1] Cycloadditions. The above mechanistic information is helpful for designing [4 + 2 + 1] cycloadditions using the aforementioned strategies of **CDS** and **SDS**. One suggestion is to find appropriate catalysts or substrates to favor the DOWN CO insertion, which will give [4 + 2 + 1] products rather than [2 + 2 + 1] products. The second suggestion is to find appropriate catalysts or substrates to prefer [4 + 2 + 1] reductive elimination instead of [2 + 2 + 1] reductive elimination if the DOWN CO insertion is not favored compared to the UP CO insertion. In both cases, keeping the rhodium centers to be 16-electron in the corresponding transition states of the UP CO insertion pathway or reductive elimination transition state in the DOWN CO insertion pathway could be the most critical consideration. We are currently following these insights to design new [4 + 2 + 1] reactions.

Understanding Why the [4 + 2] Cycloaddition Is Disfavored. Complex **IN7** can undergo either the [4 + 2 + 1] cycloaddition by CO migratory insertion and reductive elimination (intermediate **IN7** to intermediate **IN8** and then to intermediate **IN10** via **TS5**) or the [4 + 2] reaction by reductive elimination via **TS12** (Scheme 5). The [4 + 2] reaction is disfavored since **TS12** is higher in terms of Gibbs free energy than **TS5** by 2.3 kcal/mol. This implies that the [4 + 2] reaction is not favored compared to [4 + 2 + 1], agreeing with experimental observations that only a trace amount of the [4 + 2] product was generated.

Here, we interpret this selectivity. The reductive elimination reaction from intermediate **IN7** requires a Gibbs free energy of activation of 17.3 kcal/mol to give the [4 + 2] product. However, this is disfavored compared to the direct coordination of **IN7** by CO (a diffusion-controlled process), forming intermediate **IN8** and then intermediate **IN9**. This CO coordination and geometry reorganization is exergonic by 5.2 kcal/mol. Intermediate **IN9** then undergoes CO insertion with a Gibbs free energy of activation of 20.3 kcal/mol via **TS5**. Certainly, intermediate **IN9** can also go back to intermediate **IN7** and release a CO molecule, with a Gibbs free energy of activation of 12.6 kcal/mol, which is estimated by the direct free energy difference between intermediates **IN8** and **IN9**. This suggests that intermediates **IN7**, **IN8**, and **IN9** are in equilibrium, and the regiochemistry is determined by the relative energy of **TS5** and **TS12**, according to the Curtin−Hammett principle. Consequently, the [4 + 2 + 1] pathway is preferred. Here, we point out that when CO was not added to the reaction, the substrates could undergo the [4 + 2] cycloaddition, as demonstrated by Tang.[10] The present study provides an understanding of this [4 + 2] process as well.

Understanding the Mechanism of Generation of a Side Product of the Triene by Model Reaction 5. In our previous experimental study, we found that the triene side product could be obtained when using a *Z*-configuration substrate to synthesize the [4 + 2 + 1] product (Scheme 2a). However, no triene side product was observed for the *E*-configuration substrate. Why? We used the model reaction 5 of *Z*-**1c** for a computational study to understand the possible reasons (Scheme 2b).

https://doi.org/10.1021/acs.joc.2c00406
J. Org. Chem. 2022, 87, 10576−10591

Scheme 6. [1,5]-H Shifts to Generate Trienes[a]

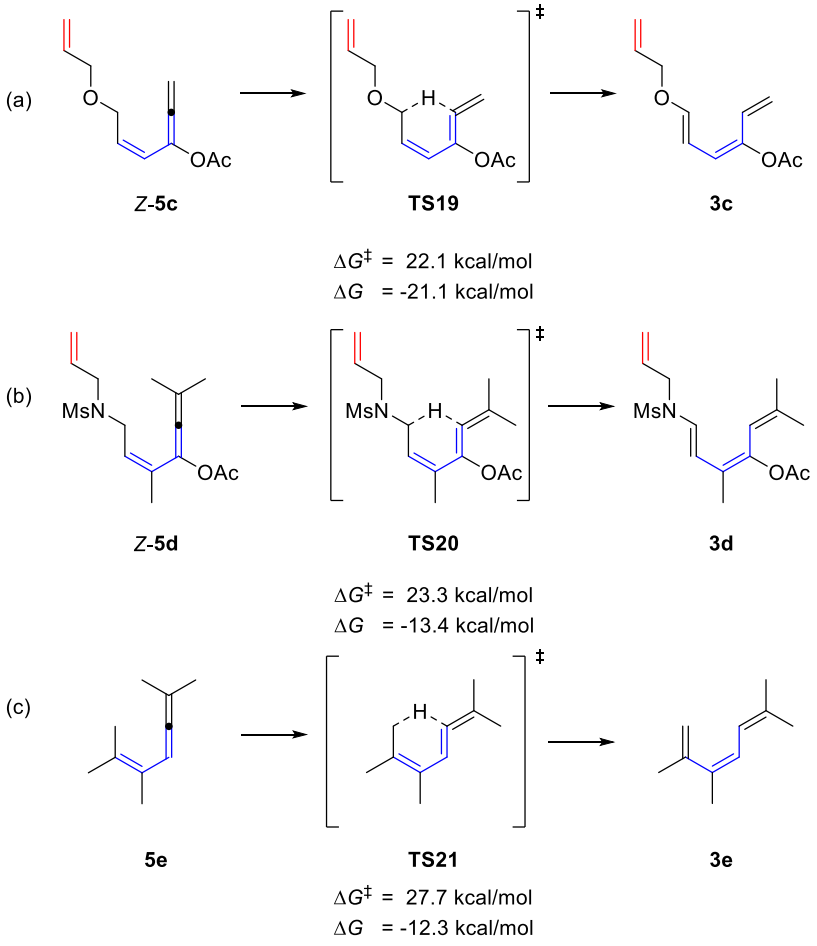

[a](a) Our simplified model system. (b) *Z*-**5d** system from *Z*-**1d** (close to the real *Z*-**1a** system shown in Scheme 2). (c) Literature reported the [1,5]-H shift process together with the computational results from this study.

Figure 9 shows the computed free energy profiles for both pathways of triene formation and [4 + 2 + 1] cycloaddition (the resting state and generation of substrate-$Rh(CO)_2Cl$ here are proposed to be similar to those processes in Figure 2). The 1,3-acyloxy migration step for the formation of intermediate **IN23** is a little slower for complex **IN21** compared to substrate *E*-**1c**, 27.0 kcal/mol vs 24.5 kcal/mol (**TS14** and **TS1**, respectively). Then, intermediate **IN23** undergoes oxidative addition (via **TS17**) of the C−H bond adjacent to the oxygen atom, giving Rh(III) intermediate **IN27**, which is a 16-electron complex. In **TS17**, the corresponding H−Rh and C−Rh bonds form, and the C−H bond breaks. This step needs 18.5 kcal/mol of Gibbs free energy to deliver intermediate **IN27**. Finally, intermediate **IN27** produces the triene as the side product, via a reductive elimination reaction. The reductive elimination via **TS18** requires an activation free energy of 7.2 kcal/mol. The rate-determining step in triene production is the oxidative addition of the C−H bond via **TS17**.

In the [4 + 2 + 1] pathway, intermediate **IN23** (a 16-electron intermediate) can form an 18-electron intermediate **IN24** through geometry changes. **IN24** then dissociates a CO molecule to generate intermediate **IN25**. Subsequently, intermediate **IN25** will be converted to intermediate **IN26**, which can undergo oxidative cyclization to form intermediate **IN7**, which is the same intermediate for the [4 + 2 + 1] reaction from *E*-**1c** shown in Figure 2. In Figure 9, **TS15** of CO dissociation was also estimated, similar to that of **TS3** in Figure 2.

Unfortunately, the proposed pathway of the triene generation in Figure 9 is disfavored compared to the [4 + 2 + 1] reaction pathway, because **TS17** is 5.8 kcal/mol higher than **TS15**, suggesting that no triene is generated. These calculation results did not agree with the experiments. One reason for the discrepancy could be the simplification of model calculations. However, using the model reaction 6 with substrate **1d** (Scheme 2, **1d** is different from the real substrate by the Ns group, which is expected to be trivial for affecting the computational results) gave a similar conclusion (see the Supporting Information for more discussion).

Therefore, we proposed that once **IN23** is generated, it can then isomerize to **IN24**. Both **IN23** and **IN24** could undergo ligand exchange with the solvent, substrate, or product to give free ene−allene *Z*-**5c**, which then can undergo a [1,5]-H shift, with a computed activation free energy of 22.1 kcal/mol, to deliver the triene (Scheme 6a). For **1d**, the activation free energy for free ene−allene *Z*-**5d** is 23.3 kcal/mol (Scheme 6b). A similar [1,5]-H shift has been observed by Okamura[24a] and Braverman[24b] and the computed activation free energy for their substrate in the present study is 27.7 kcal/mol (experimentally, this reaction occurred at refluxed chloroform). The details for the dissociation of the catalyst from **IN23** are not known and we, therefore, cannot compute its kinetic value

https://doi.org/10.1021/acs.joc.2c00406
J. Org. Chem. 2022, 87, 10576−10591

to determine the ratio of the triene with respect to the [4 + 2 + 1] cycloadduct. But we can estimate that this process has an activation free energy of 18.0 kcal/mol, close to the energy difference of **TS15** and **IN24**, considering that the ratio of the triene and [4 + 2 + 1] product was 1/10 for reaction 1 in Scheme 2. More discussions of reaction 6 are given in the Supporting Information.

For the substrate *E*-**1c**, dissociation of Rh from intermediate **IN4** is also possible, but this will not generate the triene because a [1,5]-H shift is not allowed geometrically: **IN4** has a *trans* configuration of its central ene. Therefore, for ene−ene−propargylic ester substrates with an *E*-configuration, no triene products were observed in these substrates. Based on these, we propose that trienes are generated by (metal-free) direct [1,5]-H shift reactions after 1,3-acyloxy migration.

The present [4 + 2 + 1] reaction of *Z*-**1c** has the 1,3-acyloxy migration as the rate-determining step (26.8 kcal/mol from 1/2$[Rh(CO)_2Cl]_2$ and the substrate to **TS14**, Figure 9). The overall activation energy is not known because we do not know the exact form of the resting state.

Revision of the Geometry of the Triene Side Products. Finally, we point out that we originally proposed that trienes have an *trans*-configuration (with respect to the connected two vinyl groups) in their middle alkene moieties.[6a] From the present mechanistic study, we now revise the structures of these trienes, which have a *cis*-configuration for their middle alkenes, as shown in all related figures and schemes in this paper. This correction is further supported by the NOESY study of one triene product, which is present in the Supporting Information.

CONCLUSIONS

The mechanism of the rhodium-catalyzed [4 + 2 + 1] cycloaddition of ene−ene−propargylic esters and CO has been investigated by visual kinetics and quantum chemistry calculations. This study is not only important to understand how this reaction takes place, but is also helpful for guiding the future design of new [4 + 2 + 1] reactions through designing catalysts and/or substrates. Calculations showed that the [4 + 2 + 1] reaction starts with the 1,3-acyloxy migration of its ester group to form an allene intermediate (rate-determining). Then, CO dissociation and an oxidative cyclization into the Rh−C bond give a 5/7 rhodacyclic ring, which is followed by a CO migratory insertion step and reductive elimination (Figure 2).

There are two key steps influencing regiochemistry to give either [4 + 2 + 1] or [2 + 2 + 1] products. The first step affecting regiochemistry is the CO insertion into the seven-membered rhodacycle intermediate. The UP CO insertion, in which the CO insertion transition state has additional coordination from the alkene double bond of the rhodacycle intermediate, is favored compared to the DOWN CO insertion, in which the CO insertion transition state is a 14-electron complex and is disfavored energetically. The main reason for excluding the DOWN CO insertion pathway is the reductive elimination transition state to [4 + 2 + 1] product in this pathway is energetically higher than the CO insertion transition state in the UP CO insertion pathway. The DOWN CO insertion would only give the [4 + 2 + 1] product. Therefore, these regiochemistry insights imply that the future design of new [4 + 2 + 1] reactions could select appropriate catalysts or substrates by introducing additional groups to coordinate with the transition metal and make DOWN CO insertion become easier. In the reaction of ene−ene−allenes and CO, there is no such substituent to achieve this coordination and consequently, the UP CO insertion is favored.

The second step affecting regiochemistry is the reductive elimination step in the UP CO insertion pathway (in the case of the DOWN CO insertion being impossible). The [4 + 2 + 1] formation transition state with additional allene coordination from the rhodacycle is a 16-electron complex, which is more favored than the 14-electron complex of the [2 + 2 + 1] transition state without allene coordination. Therefore, the future design of the [4 + 2 + 1] reaction could introduce some groups that help the [4 + 2 + 1] pathway by keeping the reductive elimination transition state to be 16-electron. In the reaction of ene−ene−allenes and CO, the allene group plays such a role in coordination, which leads to the preference for the [4 + 2 + 1] reaction.

Other side reactions of [4 + 2], [4 + 1], and the generation of trienes have also been studied and many insights (for example, trienes are generated through [1,5]-H shifts) have been revealed in this study. We expect that these insights could serve as mechanistic guidance for designing new [4 + 2 + 1] cycloadditions and other reactions as well.

ASSOCIATED CONTENT

Supporting Information

The Supporting Information is available free of charge at https://pubs.acs.org/doi/10.1021/acs.joc.2c00406.

More discussion and computational details; kinetic study; and correction of the structure of the triene product by NOESY (PDF)

AUTHOR INFORMATION

Corresponding Author

Zhi-Xiang Yu − *Beijing National Laboratory for Molecular Sciences (BNLMS), Key Laboratory of Bioorganic Chemistry and Molecular Engineering of Ministry of Education, College of Chemistry, Peking University, Beijing 100871, China;* orcid.org/0000-0003-0939-9727; Email: yuzx@pku.edu.cn

Authors

Yusheng Yang − *Beijing National Laboratory for Molecular Sciences (BNLMS), Key Laboratory of Bioorganic Chemistry and Molecular Engineering of Ministry of Education, College of Chemistry, Peking University, Beijing 100871, China*

Zi-You Tian − *Beijing National Laboratory for Molecular Sciences (BNLMS), Key Laboratory of Bioorganic Chemistry and Molecular Engineering of Ministry of Education, College of Chemistry, Peking University, Beijing 100871, China*

Chen-Long Li − *Beijing National Laboratory for Molecular Sciences (BNLMS), Key Laboratory of Bioorganic Chemistry and Molecular Engineering of Ministry of Education, College of Chemistry, Peking University, Beijing 100871, China*

Complete contact information is available at: https://pubs.acs.org/10.1021/acs.joc.2c00406

Author Contributions

†Y.Y. and Z.-Y.T. contributed equally.

Notes

The authors declare no competing financial interest.

https://doi.org/10.1021/acs.joc.2c00406
J. Org. Chem. 2022, 87, 10576−10591

■ ACKNOWLEDGMENTS

This work was supported by the National Natural Science Foundation of China (21933003) and the High-Performance Computing Platform of Peking University.

■ REFERENCES

(1) For selected reviews: (a) Wang, J.; Blaszczyk, S. A.; Li, X.; Tang, W. Transition Metal-Catalyzed Selective Carbon-Carbon Bond Cleavage of Vinylcyclopropanes in Cycloaddition Reactions. *Chem. Rev.* **2021**, *121*, 110−139. (b) Sokolova, O. O.; Bower, J. F. Selective Carbon−Carbon Bond Cleavage of Cyclopropylamine Derivatives. *Chem. Rev.* **2021**, *121*, 80−109. (c) Wang, L.-N.; Yu, Z.-X. Transition-Metal-Catalyzed Cycloadditions for the Synthesis of Eight-Membered Carbocycles: an Update from 2010 to 2020. *Chin. J. Org. Chem.* **2020**, *40*, 3536−3558. (d) Trost, B. M.; Zuo, Z.; Schultz, J. E. Transition-Metal-Catalyzed Cycloaddition Reactions to Access Seven-Membered Rings. *Chem. − Eur. J.* **2020**, *26*, 15354−15377. (e) Blaszczyk, S. A.; Glazier, D. A.; Tang, W. Rhodium-Catalyzed (5 + 2) and (5 + 1) Cycloadditions Using 1,4-Enynes as Five-Carbon Building Blocks. *Acc. Chem. Res.* **2020**, *53*, 231−243. (f) Yang, S.; Shi, M. Recent Advances in Transition-Metal-Catalyzed/Mediated Transformations of Vinylidenecyclopropanes. *Acc. Chem. Res.* **2018**, *51*, 1667−1680. (g) Souillart, L.; Cramer, N. Catalytic C−C Bond Activations via Oxidative Addition to Transition Metals. *Chem. Rev.* **2015**, *115*, 9410−9464. (h) Jiao, L.; Yu, Z.-X. Vinylcyclopropane Derivatives in Transition-Metal-Catalyzed Cycloadditions for the Synthesis of Carbocyclic Compounds. *J. Org. Chem.* **2013**, *78*, 6842−6848. (i) Pellissier, H. Recent Developments in the [5 + 2] Cycloaddition. *Adv. Synth. Catal.* **2011**, *353*, 189−218. (j) Yu, Z.-X.; Wang, Y.; Wang, Y. Transition-Metal-Catalyzed Cycloadditions for the Synthesis of Eight-Membered Carbocycles. *Chem. − Asian J.* **2010**, *5*, 1072−1088. (k) Harmata, M. The (4+3)-Cycloaddition Reaction: Simple Allylic Cations as Dienophiles. *Chem. Commun.* **2010**, *46*, 8886−8903. (l) Butenschön, H. Seven-Membered Rings by Cyclization at Transition Metals: [4+3], [3+2+2], [5 + 2]. *Angew. Chem., Int. Ed.* **2008**, *47*, 5287−5290. (m) Rubin, M.; Rubina, M.; Gevorgyan, V. Transition Metal Chemistry of Cyclopropenes and Cyclopropanes. *Chem. Rev.* **2007**, *107*, 3117−3179. (n) Lautens, M.; Klute, W.; Tam, W. Transition Metal-Mediated Cycloaddition Reactions. *Chem. Rev.* **1996**, *96*, 49−92.

(2) (a) de Oliveira, K. T.; Servilha, B. M.; de Alves, L. C.; Desiderá, A. L.; Brocksom, T. J. The Synthesis of Seven-Membered Rings in Natural Products. In *Studies in Natural Products Chemistry*, Atta ur, R., Ed.; Elsevier, 2014; Vol. *42*, pp 421−463. (b) Battiste, M. A.; Pelphrey, P. M.; Wright, D. L. The Cycloaddition Strategy for the Synthesis of Natural Products Containing Carbocyclic Seven-Membered Rings. *Chem. − Eur. J.* **2006**, *12*, 3438−3447. (c) Liu, N.; Song, W.; Schienebeck, C. M.; Zhang, M.; Tang, W. Synthesis of Naturally Occurring Tropones and Tropolones. *Tetrahedron* **2014**, *70*, 9281−9305.

(3) For selected recent reactions: (a) Li, C.-L.; Yang, Y.; Zhou, Y.; Yu, Z.-X. A Formal [3+3+1] Reaction of Enyne-Methylenecyclopropanes through Au(I)-Catalyzed Enyne Cycloisomerization and Rh(I)-Catalyzed [6+1] Reaction of Vinylspiropentanes and CO. *Asian J. Org. Chem.* **2022**, *11*, No. e202100571. (b) Arai, N.; Ohkuma, T. Stereoselective Construction of Cycloheptene-Fused Indoline Frameworks through Photosensitised Formal [5 + 2] Cycloaddition. *Tetrahedron Lett.* **2022**, *88*, No. 153588. (c) Zhang, R.; Xia, Y.; Dong, G. Intermolecular [5 + 2] Annulation between 1-Indanones and Internal Alkynes by Rhodium-Catalyzed C−C Activation. *Angew. Chem., Int. Ed.* **2021**, *60*, 20476−20482. (d) Chai, W.; Zhou, Q.; Ai, W.; Zheng, Y.; Qin, T.; Xu, X.; Zi, W. Lewis-Acid-Promoted Ligand-Controlled Regiodivergent Cycloaddition of Pd-Oxyallyl with 1,3-Dienes: Reaction Development and Origins of Selectivities. *J. Am. Chem. Soc.* **2021**, *143*, 3595−3603. (e) Evans, P. A.; Dushnicky, M. J.; Cho, D.; Majhi, J.; Choi, S.; Pipaliya, B. V.; Inglesby, P. A.; Baik, M.-H. Diastereoselective Rhodium-Catalyzed [(3+2+2)] Carbocyclization Reactions with Tethered Alkynylidenecyclopropanes: Synthesis of the Tremulane Sesquiterpene Natural Products. *Asian J. Org. Chem.* **2021**, *10*, 2174−2183.

(4) (a) Wender, P. A.; Deschamps, N. M.; Gamber, G. G. The Dienyl Pauson-Khand Reaction. *Angew. Chem., Int. Ed.* **2003**, *42*, 1853−1857. (b) Wender, P. A.; Croatt, M. P.; Deschamps, N. M. Rhodium(I)-Catalyzed [2 + 2 + 1] Cycloadditions of 1,3-Dienes, Alkenes, and CO. *J. Am. Chem. Soc.* **2004**, *126*, 5948−5949. (c) Wender, P. A.; Croatt, M. P.; Deschamps, N. M. Metal-Catalyzed [2 + 2 + 1] Cycloadditions of 1,3-Dienes, Allenes, and CO. *Angew. Chem., Int. Ed.* **2006**, *45*, 2459−2462. (d) Croatt, M. P.; Wender, P. A. The Diene Effect: The Design, Development, and Mechanistic Investigation of Metal-Catalyzed Diene-yne, Diene-ene, and Diene-allene [2 + 2 + 1] Cycloaddition Reactions. *Eur. J. Org. Chem.* **2010**, *2010*, 19−32.

(5) For other types of [4 + 2 + 1] reactions and mechanistic studies, see (a) Ni, Y.; Montgomery, J. An Efficient [4 + 2 + 1] Entry to Seven-Membered Rings. *J. Am. Chem. Soc.* **2004**, *126*, 11162−11163. (b) Ni, Y.; Montgomery, J. Synthetic Studies and Mechanistic Insight in Nickel-Catalyzed [4 + 2 + 1] Cycloadditions. *J. Am. Chem. Soc.* **2006**, *128*, 2609−2614. (c) Wang, Y.-J.; Li, X.-X.; Chen, Z. Gold-Catalyzed Diastereoselective Formal Intermolecular [4 + 2 + 1] Cycloaddition of 1,3-Dien-8-yne with Diazo Ester. *J. Org. Chem.* **2020**, *85*, 7694−7703. (d) Lv, K.; Bao, X. Mechanistic Insights into Nickel- and Gold-Catalyzed Diastereoselective [4 + 2 + 1] Cycloadditions between Dienynes and Diazo Compounds: a DFT Study. *Org. Chem. Front.* **2022**, *9*, 693−702. (e) Sasaki, I.; Ohmura, T.; Suginome, M. Construction of Silicon-Containing Seven-Membered Rings by Catalytic [4 + 2 + 1] Cycloaddition through Rhodium Silylenoid. *Org. Lett.* **2020**, *22*, 2961−2966. (f) Herndon, J. W.; Chatterjee, G.; Patel, P. P.; Matasi, J. J.; Turner, S. U.; Harp, J. J.; Reid, M. D. Cyclopropylcarbene-Tungsten Complexes + Alkynes: a [4 + 2 + 1] Cycloaddition Route for the Construction of Seven-Membered Rings. *J. Am. Chem. Soc.* **1991**, *113*, 7808−7809.

(6) (a) Tian, Z.-Y.; Cui, Q.; Liu, C.-H.; Yu, Z.-X. Rhodium-Catalyzed [4 + 2 + 1] Cycloaddition of In Situ Generated Ene/Yne-Ene-Allenes and CO. *Angew. Chem., Int. Ed.* **2018**, *57*, 15544−15548. (b) Cui, Q.; Tian, Z.-Y.; Yu, Z.-X. Rhodium(I)-Catalyzed Three-Component [4 + 2 + 1] Cycloaddition of Two Vinylallenes and CO. *Chem. − Eur. J.* **2021**, *27*, 5638−5641.

(7) (a) Shu, X. Z.; Shu, D.; Schienebeck, C. M.; Tang, W. Rhodium-Catalyzed Acyloxy Migration of Propargylic Esters in Cycloadditions, Inspiration from the Recent "Gold Rush. *Chem. Soc. Rev.* **2012**, *41*, 7698−7711. (b) Shu, X. Z.; Schienebeck, C. M.; Song, W.; Guzei, I. A.; Tang, W. Transfer of Chirality in the Rhodium-Catalyzed Intramolecular [5 + 2] Cycloaddition of 3-Acyloxy-1,4-enynes (ACEs) and Alkynes: Synthesis of Enantioenriched Bicyclo[5.3.0]-decatrienes. *Angew. Chem., Int. Ed.* **2013**, *52*, 13601−13605. (c) Ke, X.-N.; Schienebeck, C. M.; Zhou, C.-C.; Xu, X.-F.; Tang, W.-P. Mechanism and Reactivity of Rhodium-Catalyzed Intermolecular [5 + 1] Cycloaddition of 3-Acyloxy-1,4-enyne (ACE) and CO: a Computational Study. *Chin. Chem. Lett.* **2015**, *26*, 730−734. (d) Xu, X.; Liu, P.; Shu, X.-Z.; Tang, W.; Houk, K. N. Rh-Catalyzed (5 + 2) Cycloadditions of 3-Acyloxy-1,4-enynes and Alkynes: Computational Study of Mechanism, Reactivity, and Regioselectivity. *J. Am. Chem. Soc.* **2013**, *135*, 9271−9274. (e) Coskun, D.; Tüzün, N. Ş. A DFT Study on the Mechanism of Rh-Catalyzed Competitive 1,2- versus 1,3-Acyloxy Migration Followed by [5+1] and [4+1] Cycloadditions of 1,4-Enynes with CO. *J. Organomet. Chem.* **2017**, *851*, 97−103. (f) Shu, D.; Li, X.; Zhang, M.; Robichaux, P. J.; Guzei, I. A.; Tang, W. Rhodium-Catalyzed Carbonylation of Cyclopropyl Substituted Propargyl Esters: A Tandem 1,3-Acyloxy Migration [5 + 1] Cycloaddition. *J. Org. Chem.* **2012**, *77*, 6463−6472. (g) Li, X.; Huang, S.; Schienebeck, C. M.; Shu, D.; Tang, W. Rhodium-Catalyzed Carbonylation of 3-Acyloxy-1,4-Enynes for the Synthesis of Cyclopentenones. *Org. Lett.* **2012**, *14*, 1584−1587. (h) Coskun, D.; Tüzün, N. S. A DFT Study on the Mechanism of Rh-Catalyzed Competitive 1,2- versus 1,3-Acyloxy Migration Followed by [5+1] and [4+1] Cycloadditions of 1,4-Enynes with CO. *J. Organomet. Chem.* **2017**, *851*, 97−103. (i) Jiang, J.; Liu, Y.; Hou, C.; Li, Y.; Luan,

Z.; Zhao, C.; Ke, Z. Rationalization of the Selectivity between 1,3- and 1,2-Migration: a DFT Study on Gold(i)-Catalyzed Propargylic Ester Rearrangement. *Org. Biomol. Chem.* **2016**, *14*, 3558−3563.
(8) (a) Chen, W.; Tay, J.-H.; Yu, X.-Q.; Pu, L. Diastereoselective [4 + 1] Cycloaddition of Alkenyl Propargyl Acetates with CO Catalyzed by $[RhCl(CO)_2]_2$. *J. Org. Chem.* **2012**, *77*, 6215−6222. (b) Murakami, M.; Itami, K.; Ito, Y. Rhodium-Catalyzed Asymmetric [4+1] Cycloaddition. *J. Am. Chem. Soc.* **1997**, *119*, 2950−2951. (c) Murakami, M.; Itami, K.; Ito, Y. Catalytic Asymmetric [4 + 1] Cycloaddition of Vinylallenes with Carbon Monoxide: Reversal of the Induced Chirality by the Choice of Metal. *J. Am. Chem. Soc.* **1999**, *121*, 4130−4135. (d) Murakami, M.; Itami, K.; Ito, Y. Synthesis of (Vinylallene)rhodium(III) Complex of Planar Structure: Perfect $\pi \rightarrow \sigma$ Conversion of 1,3-Diene System. *J. Am. Chem. Soc.* **1996**, *118*, 11672−11673.
(9) For selected Rh-catalyzed [4 + 2] reactions of dienes with alkynes/alkenes and mechanistic studies: (a) Gilbertson, S. R.; Hoge, G. S. Rhodium Catalyzed Intramolecular [4 + 2] Cycloisomerization Reactions. *Tetrahedron Lett.* **1998**, *39*, 2075−2078. (b) Wang, B.; Cao, P.; Zhang, X. An Efficient Rh-Catalyst System for the Intramolecular [4 + 2] and [5 + 2] Cycloaddition Reactions. *Tetrahedron Lett.* **2000**, *41*, 8041−8044. (c) Wang, B.; Cao, P.; Zhang, X. An Efficient Rh-Catalyst System for the Intramolecular [4 + 2] and [5 + 2] Cycloaddition Reactions. *Tetrahedron Lett.* **2000**, *41*, 8041−8044. (d) O'Mahony, D. J. R.; Belanger, D. B.; Livinghouse, T. Substrate Control of Stereoselection in the Rhodium(I) Catalyzed Intramolecular [4 + 2] Cycloaddition Reaction. *Org. Biomol. Chem.* **2003**, *1*, 2038−2040. (e) Motoda, D.; Kinoshita, H.; Shinokubo, H.; Oshima, K. Phosphane-Free Rhodium Catalyst in an Anionic Micellar System for [4 + 2] Annulation of Dienynes. *Angew. Chem., Int. Ed.* **2004**, *43*, 1860−1862. (f) Aikawa, K.; Akutagawa, S.; Mikami, K. Asymmetric Synergy between Chiral Dienes and Diphosphines in Cationic Rh(I)-Catalyzed Intramolecular [4 + 2] Cycloaddition. *J. Am. Chem. Soc.* **2006**, *128*, 12648−12649. (g) Shintani, R.; Sannohe, Y.; Tsuji, T.; Hayashi, T. A Cationic Rhodium−Chiral Diene Complex as a High-Performance Catalyst for the Intramolecular Asymmetric [4 + 2] Cycloaddition of Alkyne-1,3-Dienes. *Angew. Chem., Int. Ed.* **2007**, *46*, 7277−7280. (h) Falk, A.; Fiebig, L.; Neudörfl, J.-M.; Adler, A.; Schmalz, H.-G. Rhodium-Catalyzed Enantioselective Intramolecular [4 + 2] Cycloaddition Using a Chiral Phosphine-Phosphite Ligand: Importance of Microwave-Assisted Catalyst Conditioning. *Adv. Synth. Catal.* **2011**, *353*, 3357−3362. (i) Liao, W.; Yu, Z.-X. DFT Study of the Mechanism and Stereochemistry of the Rh(I)-Catalyzed Diels−Alder Reactions between Electronically Neutral Dienes and Dienophiles. *J. Org. Chem.* **2014**, *79*, 11949−11960.
(10) Huang, S.; Li, X.; Lin, C. L.; Guzeic, I. A.; Tang, W. Rhodium-Catalyzed 1,3-Acyloxy Migration and Subsequent Intramolecular [4 + 2] Cycloaddition of Vinylallene and Unactivated Alkyne. *Chem. Commun.* **2012**, *48*, 2204−2206.
(11) Frisch, M. J.; Trucks, G. W.; Schlegel, H. B.; Scuseria, G. E.; Robb, M. A.; Cheeseman, J. R.; Scalmani, G.; Barone, V.; Mennucci, B.; Petersson, G. A.; Nakatsuji, H.; Caricato, M.; Li, X.; Hratchian, H. P.; Izmaylov, A. F.; Bloino, J.; Zheng, G.; Sonnenberg, J. L.; Hada, M.; Ehara, M.; Toyota, K.; Fukuda, R.; Hasegawa, J.; Ishida, M.; Nakajima, T.; Honda, Y.; Kitao, O.; Nakai, H.; Vreven, T.; Montgomery, J. A.; Peralta, J. E., Jr.; Ogliaro, F.; Bearpark, M.; Heyd, J. J.; Brothers, E.; Kudin, K. N.; Staroverov, V. N.; Keith, T.; Kobayashi, R.; Normand, J.; Raghavachari, K.; Rendell, A.; Burant, J. C.; Iyengar, S. S.; Tomasi, J.; Cossi, M.; Rega, N.; Millam, J. M.; Klene, M.; Knox, J. E.; Cross, J. B.; Bakken, V.; Adamo, C.; Jaramillo, J.; Gomperts, R.; Stratmann, R. E.; Yazyev, O.; Austin, A. J.; Cammi, R.; Pomelli, C.; Ochterski, J. W.; Martin, R. L.; Morokuma, K.; Zakrzewski, V. G.; Voth, G. A.; Salvador, P.; Dannenberg, J. J.; Dapprich, S.; Daniels, A. D.; Farkas, Ö.; Foresman, J. B.; Ortiz, J. V.; Cioslowski, J.; Fox, D. J. *Gaussian 09*, revision E.01; Gaussian, Inc.: Wallingford, CT, 2013.
(12) (a) Riplinger, C.; Neese, F. An Efficient and Near Linear Scaling Pair Natural Orbital Based Local Coupled Cluster Method. *J. Chem. Phys.* **2013**, *138*, No. 034106. (b) Riplinger, C.; Sandhoefer, B.; Hansen, A.; Neese, F. Natural Triple Excitations in Local Coupled Cluster Calculations with Pair Natural Orbitals. *J. Chem. Phys.* **2013**, *139*, No. 134101.
(13) (a) Neese, F. The ORCA Program System. *Wiley Interdiscip. Rev.: Comput. Mol. Sci.* **2012**, *2*, 73−78. (b) Neese, F. Software Update: The ORCA Program System, Version 4.0. *Wiley Interdiscip. Rev.: Comput. Mol. Sci.* **2017**, *8*, No. e1327.
(14) Boese, A. D.; Martin, J. M. L. Development of Density Functionals for Thermochemical Kinetics. *J. Chem. Phys.* **2004**, *121*, 3405−3416.
(15) (a) Weigend, F.; Ahlrichs, R. Balanced Basis Sets of Split Valence, Triple Zeta Valence and Quadruple Zeta Valence Quality for H to Rn: Design and Assessment of Accuracy. *Phys. Chem. Chem. Phys.* **2005**, *7*, 3297−3305. (b) Andrae, D.; Häußermann, U.; Dolg, M.; Stoll, H.; Preuß, H. Energy-Adjusted Ab Initio Pseudopotentials for the Second and Third Row Transition Elements. *Theor. Chim. Acta* **1990**, *77*, 123−141.
(16) Wang, Y.; Liao, W.; Wang, Y.; Jiao, L.; Yu, Z.-X. Mechanism and Stereochemistry of Rhodium-Catalyzed [5 + 2 + 1] Cycloaddition of Ene-Vinylcyclopropanes and Carbon Monoxide Revealed by Visual Kinetic Analysis and Quantum Chemical Calculations. *J. Am. Chem. Soc.* **2022**, *144*, 2624−2636.
(17) Marenich, A. V.; Cramer, C. J.; Truhlar, D. G. Universal Solvation Model Based on Solute Electron Density and on a Continuum Model of the Solvent Defined by the Bulk Dielectric Constant and Atomic Surface Tensions. *J. Phys. Chem. B* **2009**, *113*, 6378−6396.
(18) Skirrow, F. W. Über die Löslichkeit von Kohlenoxyd in binären organischen Gemischen. *Z. Phys. Chem.* **1902**, *41U*, 139.
(19) Keith, J. A.; Carter, E. A. Quantum Chemical Benchmarking, Validation, and Prediction of Acidity Constants for Substituted Pyridinium Ions and Pyridinyl Radicals. *J. Chem. Theory Comput.* **2012**, *8*, 3187−3206.
(20) Legault, C. Y. *CYLview20*; Université de Sherbrooke: Quebec, Canada, http://www.cylview.org, 2020.
(21) (a) Burés, J. A Simple Graphical Method to Determine the Order in Catalyst. *Angew. Chem., Int. Ed.* **2016**, *55*, 2028−2031. (b) Burés, J. Variable Time Normalization Analysis: General Graphical Elucidation of Reaction Orders from Concentration Profiles. *Angew. Chem., Int. Ed.* **2016**, *55*, 16084−16087.
(22) (a) Koga, N.; Jin, S. J.; Morokuma, K. Rearrangement through Berry Pseudorotation and Olefin Insertion of d^8 Five-Coordinate $Rh(H)(C_2H_4)(CO)_2(PH_3)$. An Ab Initio MO Study. *J. Am. Chem. Soc.* **1988**, *110*, 3417−3425. (b) Matsubara, T.; Koga, N.; Ding, Y.; Musaev, D. G.; Morokuma, K. Ab Initio MO Study of the Full Cycle of Olefin Hydroformylation Catalyzed by a Rhodium Complex, $RhH(CO)_2(PH_3)_2$. *Organometallics* **1997**, *16*, 1065−1078.
(23) Wang, Y.; Wang, J.; Su, J.; Huang, F.; Jiao, L.; Liang, Y.; Yang, D.; Zhang, S.; Wender, P. A.; Yu, Z.-X. A Computationally Designed Rh(I)-Catalyzed Two-Component [5 + 2 + 1] Cycloaddition of Ene-vinylcyclopropanes and CO for the Synthesis of Cyclooctenones. *J. Am. Chem. Soc.* **2007**, *129*, 10060−10061.
(24) (a) Knudsen, C. G.; Chandraratna, R. A. S.; Walkeapaa, L. P.; Chauhan, Y. S.; Carey, S. C.; Cooper, T. M.; Birge, R. R.; Okamura, W. H. Thermal Sigmatropic Rearrangements of Vinylallenes Leading to 11-cis-Retinoids and the Novel Properties of 9-cis, 11-cis, 13-cis-Retinal and 11-cis, 13-cis-Retinal. *J. Am. Chem. Soc.* **1983**, *105*, 1626−1631. (b) Braverman, S.; Freund, M.; Reisman, D.; Goldberg, I. Synthetic Applications of the Carbanion Walk Mechanism: a Novel and Facile Method for the Preparation of 1,3-Dimethylenecyclobutane and Conjugated Vinylallene Derivatives. *Tetrahedron Lett.* **1986**, *27*, 1297−1300.

https://doi.org/10.1021/acs.joc.2c00406
J. Org. Chem. 2022, 87, 10576−10591